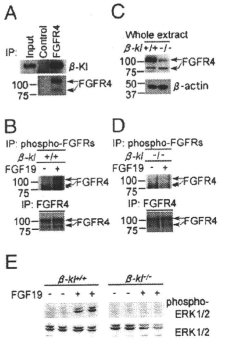

Fig. 3. FGFR4 binds to β-Kl and is phosphorylated by FGF19 in liver. (*A*) Liver lysates were precipitated with anti-FGFR4 antibody or with control IgG. Input is 1% of the liver whole extract used for the immunoprecipitation. The immunoprecipitates were separated by SDS/PAGE and blotted with anti-FGFR4 antibody. (*B*, *D*, and *E*) Ten minutes after injection of hFGF19 or control medium, livers were excised. Liver lysates from WT mice (*B*) and β-$kl^{-/-}$ mice (*D*) were immunoprecipitated with the anti–phospho-FGFRs or the polyclonal anti-FGFR4 antibody. Immunoprecipitates were blotted with anti-FGFR4 antibody. The arrowhead indicates a nonspecific band (Fig. S2). (*C*) Whole liver extracts of WT and β-$kl^{-/-}$ mice were blotted with anti-FGFR4 antibody or anti–β-actin antibody for a loading control. (*E*) Liver lysates from WT and β-$kl^{-/-}$ were immunoblotted with anti-phospho-ERK1/2 or anti-ERK1/2 antibodies ($n = 2$ in each case).

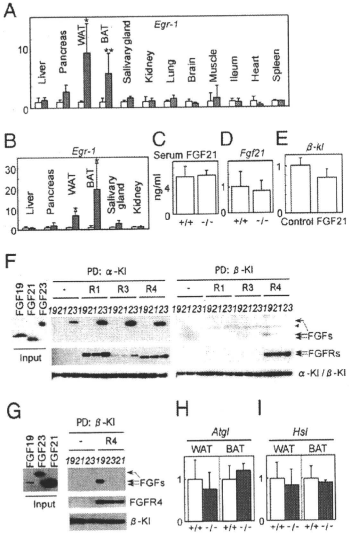

Fig. 4. β-Kl is not essential for FGF21-mediated signaling (*A–I*). Thirty minutes after injection, tissues in WT ($n = 5$/group) (*A*) and β-$kl^{-/-}$ mice ($n = 4$/group) (*B*) were excised. *Egr-1* mRNA levels were measured by RT-quantitative PCR. The expression levels of hFGF21 injected mice (*filled bars*) and vehicle injected mice (*open bars*) mice are plotted as fold change. Data were derived from 7- to 10-week-old male mice on standard diet. (*C*) Serum FGF21 concentrations of WT and β-$kl^{-/-}$ mice ($n = 5$–6/group) were measured by RIA. (*D*) *Fgf21* mRNA levels in livers of WT and β-$kl^{-/-}$ mice ($n = 5$–6/group) were measured by RT-quantitative PCR and are plotted as fold change. Data were derived from 15- to 20-week-old male mice on standard diet. hFGF21 (0.4 mg/kg) or control medium were injected into WT and β-$kl^{-/-}$ mice. (*E*) WT mice were injected with recombinant hFGF21 (0.4 mg/kg) or control medium ($n = 5$/group). Mice were killed 4 h after injection and *β-kl* mRNA levels in WAT were analyzed by RT-quantitative PCR. Data were derived from 10-week-old male mice on standard diet. (*F*) A 15-ng quantity of each FGF was pulled down (PD) by α-/β-Kl in the presence (R1, R3, or R4) or absence (–) of FGFRs. Input was 8% of samples used for the pull-down assay. Samples of pulled down by α-/β-Kl were analyzed by SDS/PAGE and blotted with antibodies (anti-His for FGFs, anti-Human Fc for FGFRs, and anti-GFP for α-/β-Kl). Arrowhead indicates a nonspecific band. (*G*) A 50-ng quantity of FGF19, 150 ng of FGF23, or 500 ng of FGF21 was precipitated by β-Kl in the presence or absence of FGFR4. Input was 1% of samples used for the assay. (*H* and *I*) *hsl* and *atgl* mRNA levels in WAT and BAT were analyzed by RT-quantitative PCR. Data were derived from 9- to 14-week-old female β-$kl^{+/+}$ and β-$kl^{-/-}$ mice ($n = 5$/group). $^*P < 0.05$; $^{**}P < 0.01$.

firmed the biological activity of the synthesized hFGF21. As shown in Fig. S5, our hFGF21 could enhance *Egr1*-derived luciferase reporter expression in a β-Kl–dependent manner at doses that were equivalent to those previously reported (17, 21). Moreover the hFGF21 up-regulated *Glut1* mRNA in 3T3-L1 adipocyte (Fig. S5) (16). Consistent with the in vitro results, in WT mice, *Egr-1* expression levels were significantly up-regulated by ~10-fold in WAT and >6-fold in BAT 30 min after injection of hFGF21 (Fig. 4*A* and Fig. S5). However, administration of hFGF21 also resulted in significant up-regulation of *Egr-1* mRNA levels in WAT and BAT from β-$kl^{-/-}$ mice (Fig. 4*B*). We next analyzed the serum levels of FGF21 and hepatic mRNA levels of *Fgf21* in WT and β-$kl^{-/-}$ mice. Unexpectedly, there was no significant genotype-dependent difference in mean serum protein concentrations of FGF21 nor hepatic *Fgf21* mRNA levels (Fig. 4 *C* and *D*). We also confirmed that *β-kl* expression was not affected by FGF21 administration (Fig. 4*E*). These results suggest that β-Kl is not essential for FGF21-mediated signaling in WAT and BAT. In addition, our prediction was further supported by the following experiments. First, to address the binding properties between β-Kl and FGF21, we performed pull-down assays using recombinant proteins. Although FGF19 was significantly bound by β-Kl in the presence of FGFR4, FGF21 could not be precipitated by β-Kl even with 10 fold amounts of FGF21 (Fig. 4 *F* and *G* and *SI Text*). Second, we compared the phenotypes of $Fgf21^{-/-}$ and β-$kl^{-/-}$ mice. Recently, Hotta et al. developed $Fgf21^{-/-}$ mice and reported that expression levels of hormone-sensitive lipase (*Hsl*) and adipose triglyceride lipase (*Atgl*) in WAT were decreased in $Fgf21^{-/-}$ mice to almost 50% compared with those of WT mice (23). The adipose phenotypes in $Fgf21^{-/-}$ mice may be an outcome of a deficiency in FGF21 signaling. Thus we analyzed the expression levels of these genes in the adipose tissues of β-$kl^{-/-}$ mice. Consequently, in both WAT and BAT, mRNA levels of *Hsl* and *Atgl* were not significantly altered between WT and β-$kl^{-/-}$ mice (Fig. 4 *H* and *I*). These data suggest that β-Kl may not necessarily be involved in the phenotypes observed in FGF21-deficient mice. Taken together, these results provide strong evidence that β-Kl is not essential for FGF21-mediated signaling in WAT and BAT. We therefore asked whether FGF21 signaling might require other unidentified components than β-Kl. We also analyzed *Glut1* mRNA levels 4 h after hFGF21 injection at concentrations that could induce *Egr-1* expression in WAT and BAT, but no apparent induction was observed, suggesting that *Glut1* is not a direct target of FGF21 signaling (28, 29).

Discussion

Various roles of Klotho family members have been reported (18, 22, 30); however, a consensus on the molecular functions of α-Kl

and β-Kl has not been reached. Based on these findings, we propose a comprehensive regulatory scheme of mineral homeostasis that is illustrated by the mutually regulated positive/negative feedback actions of α-Kl, FGF23, and $1,25(OH)_2D$ (Fig. 5*A*). In the present study, we found that FGF23 represses the expression of α-Kl and identified an essential role of α-Kl in FGF23-mediated phosphorylation of FGFR1 in the kidney. This leads to *Cyp27b1* down-regulation and *Cyp24* up-regulation, and results in inhibition of the synthesis of $1,25(OH)_2D$, an active form of vitamin D (3). $1,25(OH)_2D$ has prominent effects on the kidney, intestine, and bone. In the kidney, $1,25(OH)_2D$ activates vitamin D receptor (VDR) by binding to its ligand binding domain and negatively regulates the expression of *Cyp27b1* while positively regulating *Cyp24* and α-Kl expression (2). In the bone, $1,25(OH)_2D$ binds to VDR and induces FGF23 synthesis in osteocytes and osteoblasts (31) in hours/days. In turn, secreted FGF23 suppresses $1,25(OH)_2D$ synthesis and inorganic phosphate reabsorption in the kidney to adjust extracellular mineral concentrations. Collectively, α-Kl, in combination with FGF23, is involved in a signaling cascade that maintains extracellular calcium/phosphate levels within a narrow range.

The roles of β-Kl, FGF15, and FGFR4 in bile acid/cholesterol metabolism are schematically summarized in Fig. 5*B*. Consistent with a previous study (10, 22), i.v. injection of hFGF19 dramatically represses the expression of *Cyp7a1* and *Cyp8b1* and results in the inhibition of bile acid synthesis from cholesterol in WT livers. This suppression of *Cyp7a1* and *Cyp8b1* was not observed in *β-kl*$^{-/-}$ mice. Indeed, phosphorylation of FGFR4 and ERK1/2 was not detected in *β-kl*$^{-/-}$ livers even after hFGF19 administration. Our findings provide conclusive evidence proving the essential role of β-Kl in FGF15/hFGF19-mediated activation of FGFR4 and subsequent signal transduction that regulates bile acid synthesis. Particularly, by binding to FXR, bile acid induces SHP expression in the liver and FGF15 transcription in the terminal ileum. In turn, increased SHP and secreted FGF15 differentially suppress Cyp7a1/Cyp8b1 expression to down-regulate bile acid synthesis (8, 9, 11). In addition, we found mutual negative feedback regulations between β-Kl and FGF15, namely, a decrease in *β-kl* after hFGF19 administration and an increase in *Fgf15* in *β-kl* deficiency. In other words, *β-kl* ablation leads to impaired negative feedback regulation of bile acid metabolism, resulting in the overflow of bile acid pools. Consequently, in the *β-kl*$^{-/-}$ terminal ileum, chronic stimulation by elevated bile acid would lead to an unusual increase in *Fgf15* mRNA. We propose a scheme illustrating the bile acid/cholesterol homeostasis regulated by mutual negative/positive feedback actions of β-Kl, FGF15, and bile acids (Fig. 5*B*).

As shown in Fig. 5, the scheme for bile acid regulation by β-Kl/FGF15 is conceptually analogous to that of vitamin D metabolism, which involves α-Kl and FGF23. Both systems are regulated by the coordination of two types of feedback mechanisms mediated by end-metabolites, $1,25(OH)_2D$ or bile acids, that are in situ negative feedback regulation and target tissue mediated negative feedback loop. In the former pathway, the end-metabolite functions as a nuclear receptor ligand and negatively feeds back by repressing the expression of key regulatory enzymes (Cyp27b1 in the kidney or Cyp7a1/Cyp8b1 in the liver) in the relevant metabolic pathway responsible for the generation of end-metabolite itself. In the latter system, the end-metabolite is transported to the target tissue (bone or intestine) from a distal site and enhances the expression of FGF (FGF23 or FGF15) by binding to the nuclear receptor; VDR or FXR. Subsequently, secreted FGF acts as the regulator of a target tissue–mediated negative feedback loop in collaboration with α-Kl or β-Kl. The next question to be addressed is how these two pathways are coordinately involved in the rapid adjustment and long term maintenance of mineral homeostasis and bile acid metabolism.

In a previous report, we showed that i.v. injection of hFGF23 induces phosphorylation of ERK1/2 and specifically up-regulates the expression of *Egr-1* in the murine kidney (3). Here we demonstrate that α-Kl is required for FGF23 signal transduction in vivo. Likewise, i.v. injection of hFGF19 results in ERK1/2 phosphorylation and up-regulation of *Egr-1* in the liver in a β-Kl–dependent manner. Among β-Kl–expressing organs, significant up-regulation of *Egr-1* was observed in tissues where β-Kl and FGFR4 are coexpressed. Although induction of *Egr-1* in pancreas and WAT are slight, it occurs in a β-Kl–dependent manner. FGF15-mediated signal in pancreas and WAT could therefore be involved in bile acid homeostasis, but its functional importance has yet to be elucidated. Furthermore, the very high *Egr-1* induction in the liver strongly suggests that other elements, in addition to the coexpression of β-Kl and FGFR4, may endow this prominent hepatic signal activation. Recently, several groups have reported that α-Kl and β-Kl can bind to certain types of FGFRs. Those studies report preferences and differences for this binding that might be dependent on assay conditions. α-Kl solely binds to FGFR1(IIIc) in vitro (3), however α-Kl binds to not only FGFR1(IIIc) but also FGFR4 and weakly to FGFR3(IIIc) in cultured cells (30). Even though FGFR4 could precipitate α-Kl in the kidney, activation of FGFR4 by hFGF23 could not be detected. Further studies are required to understand how FGFR(s) is definitively and preferentially used for a particular FGF signal in vivo.

Serum levels of FGF23 and ileac *Fgf15* mRNA expression were intensively increased in *α-kl*$^{-/-}$ and *β-kl*$^{-/-}$ mice, respectively. Furthermore, administrations of hFGF23 and hFGF19 apparently suppressed the expression of *α-kl* and *β-kl*, respectively. In contrast, the serum levels of FGF21 and hepatic *Fgf21* mRNA expression were not increased in *β-kl*$^{-/-}$ mice, and *β-kl* expression was not significantly suppressed by hFGF21 in adipose. Consistent with a previous report that FGF21 induces ERK1/2 phosphorylation specifically in WAT (17), administration of FGF21 to WT mice significantly induced *Egr-1* mRNA expression in WAT and BAT, suggesting that WAT and BAT were the possible target tissues of FGF21. However, surprisingly, remarkable *Egr-1* inductions in WAT and BAT were also observed in *β-kl*$^{-/-}$ mice, indicating that β-Kl is not essential for FGF21 signal transduction in vivo. These in vivo results contrasted with those obtained from in vitro assays, as β-Kl is essential for FGF21-mediated signal transduction in vitro. We reproduced the direct binding of α-Kl and hFGF23 and also confirmed tricomplex formation of β-Kl, hFGF19, and FGFR4 but were unable to detect binding of α-/β-Kl and hFGF21 in our pull-down assay (Fig. 4*G*). Furthermore, we confirmed that the adipose phenotypes in *Fgf21*$^{-/-}$ mice did not overlap with those of *β-kl*$^{-/-}$ mice. This inconsistency leads to a postulation that β-Kl is not necessary for FGF21 signaling.

Currently, β-Kl is believed to be a common player essential for FGF15- and FGF21-mediated signal transduction. However, our present results, together with the data from Hotta et al. (23), do

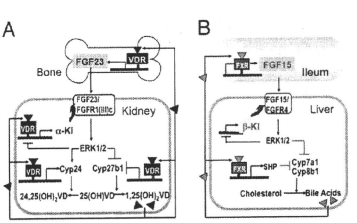

Fig. 5. Schematic representation of α-Kl/FGF23 and β-Kl/FGF15 systems. (*A*) Regulatory network of mineral homeostasis illustrated by the mutual positive/negative feedback actions of α-Kl, FGF23, and $1,25(OH)_2D$. (*B*) Regulatory network of bile acid/cholesterol metabolism represented by the mutual positive/negative feedback actions of β-Kl, FGF15, and bile acids.

not support this hypothesis. Possible explanations are that the response found in cultured cells might be caused by: (*i*) an artificial abundance of β-Kl and/or FGF21, (*ii*) peculiar characteristics of the cultured cells used in these experiments, and/or (*iii*) a combination of these two factors (17, 20, 21).

Recent studies have reported that FGF21 stimulates lipolysis in WAT and ketogenesis in the liver (32, 33). However, those results represent the pharmacological effects of sustained FGF21 treatment and thus include consequences that are secondary and indirectly induced by FGF21. We propose a β-Kl–independent response directly triggered by hFGF21 administration. Significant *Egr-1* upregulation in WAT and BAT are indicative that FGF21 mediates lipid metabolism in adipose tissues. The physiological target(s) of FGF21 signaling need to be clarified to understand how FGF21 functions as a regulator of lipid metabolism. Observations using genetic manipulation will lead us to a precise understanding of the roles of the FGF19 subfamily in metabolic homeostasis in vivo.

Materials and Methods

Measurement of Serum Parameters. Blood samples were collected from orbital cavities or hearts under anesthesia and were centrifuged to obtain sera. Serum FGF23 levels were measured by sandwich ELISA (Kainos Laboratory), which can quantify the intact form or FGF23 using human recombinant FGF23 as a standard. Serum $1,25(OH)_2D$ levels were analyzed by SRL, Inc. Serum FGF21 levels were measured by specific RIA (Phoenix Pharmaceuticals, Inc.).

Statistical Analysis. Unless otherwise noted, all values are expressed as mean ± SD. All data were analyzed by the Mann–Whitney *U* test. *P* values less than 0.05 were considered to be statistically significant.

More details are described in *SI Materials and Methods*.

ACKNOWLEDGMENTS. We thank Drs. M. Murata and R.Yu for critical reading of the manuscript and M. Terao and K. Yurugi for support in our experiments. This work was supported Ministry of Education, Science and Culture Grants 19045016 and 21390058 (to A.I.) and 17109004 (to Y-I.N.) and Ministry of Health and Welfare, and Labor Grant H16-genome-005 (to Y-I.N.).

1. Kuro-o M, et al. (1997) Mutation of the mouse Klotho gene leads to a syndrome resembling ageing. *Nature* 390:45–51.
2. Tsujikawa H, Kurotaki Y, Fujimori T, Fukuda K, Nabeshima Y (2003) Klotho, a gene related to a syndrome resembling human premature aging, functions in a negative regulatory circuit of vitamin D endocrine system. *Mol Endocrinol* 17:2393–2403.
3. Urakawa I, et al. (2006) Klotho converts canonical FGF receptor into a specific receptor for FGF23. *Nature* 444:770–774.
4. Imura A, et al. (2007) alpha-Klotho as a regulator of calcium homeostasis. *Science* 316: 1615–1618.
5. Nabeshima Y, Imura H (2008) alpha-Klotho: A regulator that integrates calcium homeostasis. *Am J Nephrol* 28:455–464.
6. Ito S, et al. (2000) Molecular cloning and expression analyses of mouse betaklotho, which encodes a novel Klotho family protein. *Mech Dev* 98:115–119.
7. Ito S, et al. (2005) Impaired negative feedback suppression of bile acid synthesis in mice lacking betaKlotho. *J Clin Invest* 115:2202–2208.
8. Russell DW (2003) The enzymes, regulation, and genetics of bile acid synthesis. *Annu Rev Biochem* 72:137–174.
9. Goodwin B, et al. (2000) A regulatory cascade of the nuclear receptors FXR, SHP-1, and LRH-1 represses bile acid biosynthesis. *Mol Cell* 6:517–526.
10. Inagaki T, et al. (2005) Fibroblast growth factor 15 functions as an enterohepatic signal to regulate bile acid homeostasis. *Cell Metab* 2:217–225.
11. Jones S (2008) Mini-review: Endocrine actions of fibroblast growth factor 19. *Mol Pharm* 5:42–48.
12. Itoh N, Ornitz DM (2004) Evolution of the Fgf and Fgfr gene families. *Trends Genet* 20:563–569.
13. Itoh N, Ornitz DM (2008) Functional evolutionary history of the mouse Fgf gene family. *Dev Dyn* 237:18–27.
14. Nishimura T, Utsunomiya Y, Hoshikawa M, Ohuchi H, Itoh N (1999) Structure and expression of a novel human FGF, FGF-19, expressed in the fetal brain. *Biochim Biophys Acta* 1444:148–151.
15. Nishimura T, Nakatake Y, Konishi M, Itoh N (2000) Identification of a novel FGF, FGF-21, preferentially expressed in the liver. *Biochim Biophys Acta* 1492:203–206.
16. Kharitonenkov A, et al. (2005) FGF-21 as a novel metabolic regulator. *J Clin Invest* 115: 1627–1635.
17. Ogawa Y, et al. (2007) BetaKlotho is required for metabolic activity of fibroblast growth factor 21. *Proc Natl Acad Sci USA* 104:7432–7437.
18. Kurosu H, et al. (2007) Tissue-specific expression of betaKlotho and fibroblast growth factor (FGF) receptor isoforms determines metabolic activity of FGF19 and FGF21. *J Biol Chem* 282:26687–26695.
19. Wu X, et al. (2007) Co-receptor requirements for fibroblast growth factor-19 signaling. *J Biol Chem* 282:29069–29072.
20. Suzuki M, et al. (2008) betaKlotho is required for fibroblast growth factor (FGF) 21 signaling through FGF receptor (FGFR) 1c and FGFR3c. *Mol Endocrinol* 22:1006–1014.
21. Kharitonenkov A, et al. (2008) FGF-21/FGF-21 receptor interaction and activation is determined by betaKlotho. *J Cell Physiol* 215:1–7.
22. Lin BC, Wang M, Blackmore C, Desnoyers LR (2007) Liver-specific activities of FGF19 require Klotho beta. *J Biol Chem* 282:27277–27284.
23. Hotta Y, et al. (2009) Fibroblast growth factor 21 regulates lipolysis in white adipose tissue but is not required for ketogenesis and triglyceride clearance in liver. *Endocrinology* 150:4625–4633.
24. Potthoff MJ, et al. (2009) FGF21 induces PGC-1alpha and regulates carbohydrate and fatty acid metabolism during the adaptive starvation response. *Proc Natl Acad Sci USA* 106:10853–10858.
25. Shimada T, et al. (2004) Targeted ablation of Fgf23 demonstrates an essential physiological role of FGF23 in phosphate and vitamin D metabolism. *J Clin Invest* 113: 561–568.
26. Powers CJ, McLeskey SW, Wellstein A (2000) Fibroblast growth factors, their receptors and signaling. *Endocr Relat Cancer* 7:165–197.
27. Yu C, et al. (2000) Elevated cholesterol metabolism and bile acid synthesis in mice lacking membrane tyrosine kinase receptor FGFR4. *J Biol Chem* 275:15482–15489.
28. Berglund ED, et al. (2009) Fibroblast growth factor 21 controls glycemia via regulation of hepatic glucose flux and insulin sensitivity. *Endocrinology* 150:4084–4093.
29. Xu J, et al. (2009) Fibroblast growth factor 21 reverses hepatic steatosis, increases energy expenditure, and improves insulin sensitivity in diet-induced obese mice. *Diabetes* 58:250–259.
30. Kurosu H, et al. (2006) Regulation of fibroblast growth factor-23 signaling by klotho. *J Biol Chem* 281:6120–6123.
31. Kolek OI, et al. (2005) 1alpha,25-Dihydroxyvitamin D3 upregulates FGF23 gene expression in bone: The final link in a renal-gastrointestinal-skeletal axis that controls phosphate transport. *Am J Physiol Gastrointest Liver Physiol* 289:G1036–G1042.
32. Inagaki T, et al. (2007) Endocrine regulation of the fasting response by PPARalpha-mediated induction of fibroblast growth factor 21. *Cell Metab* 5:415–425.
33. Badman MK, et al. (2007) Hepatic fibroblast growth factor 21 is regulated by PPARalpha and is a key mediator of hepatic lipid metabolism in ketotic states. *Cell Metab* 5:426–437.

Adipose Tissue–Specific Regulation of Angiotensinogen in Obese Humans and Mice: Impact of Nutritional Status and Adipocyte Hypertrophy

Shintaro Yasue[1], Hiroaki Masuzaki[1], Sadanori Okada[1], Takako Ishii[1], Chisayo Kozuka[1], Tomohiro Tanaka[1], Junji Fujikura[1], Ken Ebihara[1], Kiminori Hosoda[1], Akemi Katsurada[2], Naro Ohashi[2], Maki Urushihara[2], Hiroyuki Kobori[2], Naoki Morimoto[3], Takeshi Kawazoe[3], Motoko Naitoh[3], Mitsuru Okada[4], Hiroshi Sakaue[4,5], Shigehiko Suzuki[3] and Kazuwa Nakao[1]

BACKGROUND
The adipose tissue renin–angiotensin system (RAS) has been implicated in the pathophysiology of obesity and dysfunction of adipose tissue. However, neither regulation of angiotensinogen (AGT) expression in adipose tissue nor secretion of adipose tissue–derived AGT has been fully elucidated in humans.

METHODS
Human subcutaneous abdominal adipose tissue (SAT) biopsies were performed for 46 subjects with a wide range of body mass index (BMI). Considering the mRNA level of AGT and indices of body fat mass, the amount of adipose tissue–derived AGT secretion (A-AGT-S) was estimated. Using a mouse model of obesity and weight reduction, plasma AGT levels were measured with a newly developed enzyme-linked immunosorbent assay (ELISA), and the contribution of A-AGT-S to plasma AGT levels was assessed.

RESULTS
A-AGT-S was substantially increased in obese humans and the value was correlated with the plasma AGT level in mice. A-AGT-S and plasma AGT were higher in obese mice, whereas lower in mice with weight reduction. However, the AGT mRNA levels in the liver, kidney, and aorta were not altered in the mouse models. In both humans and mice, the AGT mRNA levels in mature adipocytes (MAs) were comparable to those in stromal-vascular cells. Coulter Multisizer analyses revealed that AGT mRNA levels in the MAs were inversely correlated with the average size of mature adipocytes.

CONCLUSIONS
This study demonstrates that adipose tissue–derived AGT is substantially augmented in obese humans, which may contribute considerably to elevated levels of circulating AGT. Adipose tissue–specific regulation of AGT provides a novel insight into the clinical implications of adipose tissue RAS in human obesity.

Keywords: *adipocyte size; adipose tissue; angiotensinogen; blood pressure; hypertension; obesity*

Am J Hypertens 2010; **23**:425-431

Activation of the renin–angiotensin system (RAS) is commonly observed in patients with obesity.[1,2] Angiotensin-converting enzyme (ACE) inhibitors and angiotensin II type 1 receptor (AT1R) blockers ameliorate obesity-related metabolic derangement.[3,4] Of note, Case-J trial demonstrated that a systemic blockade of RAS significantly reduced the incidence of newly occurring type 2 diabetes, notably in obese patients with hypertension.[5] Adipose tissue expresses all components of RAS (angiotensinogen (AGT), renin, ACE, AT1R, and angiotensin II type 2 receptor (AT2R)) in humans and rodents,[1] implicating adipose tissue RAS in the pathophysiology of obesity.

AGT, the only substrate of renin, is expressed in a variety of tissues.[1,2] Besides the liver, adipose tissue has recently been recognized as a considerable source of AGT.[1] A previous study demonstrated that transgenic overexpression of AGT exclusively in adipose tissue augmented circulation level of AGT and rescued hypotension and leanness seen in AGT knockout mice.[6] This observation indicates that adipose tissue–derived AGT contributes to circulating AGT level and resultant pathophysiology

[1]Department of Medicine and Clinical Science, Kyoto University Graduate School of Medicine, Kyoto, Japan; [2]Department of Physiology, and Hypertension and Renal Center of Excellence, Tulane University Health Sciences Center, New Orleans, Louisiana, USA; [3]Department of Plastic and Reconstructive Surgery, Kyoto University Graduate School of Medicine, Kyoto, Japan; [4]Division of Diabetes, Digestive, and Kidney Diseases, Department of Clinical Molecular Medicine, Kobe University Graduate School of Medicine, Kobe, Japan; [5]Department of Pharmacology, Kinki University School of Medicine, Sayama, Japan. Correspondence: Hiroaki Masuzaki (hiroaki@kuhp.kyoto-u.ac.jp)

Received 13 September 2009; first decision 3 November 2009; accepted 4 December 2009; advance online publication 7 January 2010. doi:10.1038/ajh.2009.263

of obesity-related metabolic diseases. Although some recent studies demonstrated that expression of adipose AGT is modified by adiposity in humans and rodents,[1,7,8] secretion of adipose tissue–derived AGT *per se* has not been elucidated. Therefore, the extent to which adipose tissue–derived AGT secretion (A-AGT-S) contributes to plasma AGT levels has not been clarified.

In this context, this study was designed to estimate the amount of A-AGT-S, considering the mRNA level of AGT and indices of body fat mass, and explored the potential regulation of A-AGT-S in relation to obesity by performing human adipose tissue biopsies. Furthermore, plasma AGT levels were measured using a newly developed enzyme-linked immunosorbent assay (ELISA),[9,10] and the contribution of A-AGT-S to plasma AGT in mouse models of obesity and weight reduction was assessed.

Although the mechanistic link between adipocyte size and metabolic consequences has long been of research interest,[11,12] the relationship between adipocyte hypertrophy and the expression level of AGT in adipocytes was not fully investigated in humans. Most of the previous studies have employed a histological approach for evaluating adipocyte size.[8,11] However, the distribution of adipocyte diameter is bimodal in humans,[12,13] resulting in limitations in assessing the representative size of adipocytes. In this context, size of mature adipocytes was precisely analyzed using a Coulter Multisizer,[12] and the possible relationship between adipocyte size and AGT mRNA level in adipocytes was explored in humans.

METHODS

Profile of subjects. This study was approved by the ethical committee on human research of Kyoto University Graduate School of Medicine (no. 553). Signed informed consent was obtained from all subjects. A total of 46 Japanese subjects (**Table 1**: 24 men and 22 women; body mass index (BMI): 29 ± 1.0 kg/m^2) were recruited for subcutaneous abdominal adipose tissue (SAT) biopsies. Patients who had received ACE inhibitors, AT1R blockers, thiazolidinediones, insulin, or steroid-related drugs were carefully excluded. Among the group, the serum leptin level was measured in 39 subjects (20 men and 19 women; BMI: 28 ± 1.2 kg/m^2). To examine the relationship between body fat mass and serum leptin level, 55 subjects (BMI: 27 ± 2.1 kg/m^2, range: 15–52) were recruited during the same period.

SAT biopsies. Adipose tissue biopsies were performed before controlling calorie intake and physical activity. SAT (~2 g) was removed from the periumbilical region under local anesthesia (lidocaine 1%). Samples were frozen in liquid nitrogen immediately and stored at −80 °C for total RNA extraction.

Hormone assays and clinical parameters. Blood samples were obtained at 0800 hours after an overnight fast 3 days before the adipose tissue biopsies. Serum leptin levels were measured using RIA (LINCO Research, St Louis, MO).

Real-time PCR. Total RNA was extracted using a QIAGEN RNeasy Kit (QIAGEN Japan, Tokyo, Japan). Complementary DNA was synthesized using an iScript cDNA Synthesis Kit (Bio-Rad, Hercules, CA). The mRNA level was quantified using the TaqMan PCR method with an ABI PRISM 7700 Sequence Detection System (Applied Biosystems, Foster City, CA).[14] The sequences of primers and probes for each gene are summarized in **Table 2**. Values were normalized to that of 18S rRNA (Applied Biosystems).

Obese and weight-losing mouse models. In diet-induced obese (12W DIO, $n = 6$) model experiments, 8-week-old male C57BL/6J mice were housed for 4 weeks on a high-fat/high-sucrose diet (D12493; Oriental Bio-Service, Kyoto, Japan) or regular diet (12W RD, $n = 6$) (F-2; Funahashi, Chiba, Japan). In the weight-losing (14W WL) mouse experiments, 6-week-old male C57BL/6J mice were maintained on a high-fat/high-sucrose diet for 4 weeks, then from 10 weeks of age were subjected to diet substitution from a high-fat/high-sucrose diet to an RD for 4 weeks. In addition, 6-week-old male C57BL/6J mice were maintained on high-fat/high-sucrose diet (14W DIO, $n = 6$) for 8 weeks. Experimental protocol of obese and weight-losing mouse models is schematized in **Supplementary Figure S1** online.

Estimation of A-AGT-S. The amount of A-AGT-S was estimated by multiplying the mRNA level of AGT/g adipose tissue with the weight of body fat mass. Because serum leptin level was tightly correlated with body fat mass,[15] the serum leptin levels were used as a representative index of body fat mass in humans. Estimation of A-AGT-S is schematized in **Supplementary Figure S2** online.

ELISA for AGT. AGT protein was determined using a newly developed ELISA.[9,10]

Cell culture. 3T3-L1 fibroblasts were maintained and differentiated into mature adipocytes.[14] Fully differentiated adipocytes (day 8) were exposed to 10^{-9}, 10^{-8}, or 10^{-7} mol/l dexamethasone for 48 h. Total RNA was extracted from cultured cells using TRIzol Reagent (Invitrogen, Carlsbad, CA). For protein extraction, tissue was homogenized in a radioimmune precipitation (Upstate Cell Signaling Solutions, New York, NY)

Table 1 | Profile of subjects

	n	Mean ± s.e.m.	Range
Age (years)	46	46 ± 2.1	20–74
BMI (kg/m^2)	46	29 ± 1.0	18–52
Waist circumference (cm)	46	93 ± 2.5	63–141
Serum leptin (ng/ml)	39	15 ± 2.2	1.7–68
SBP (mm Hg)	46	131 ± 2.7	94–200
DBP (mm Hg)	46	79 ± 1.5	55–108

BMI, body mass index; DBP, diastolic blood pressure; SBP, systolic blood pressure.

Table 2 | Oligonucleotide sequences for primers and probes

Gene	Forward/reverse primer Probe
Human AGT	5′GGTGGAGGGTCTCACTTTCCA3′/5′ATGGTCAGGTGGATGGTCCG3′ 5′CCCTCAACTGGATGAAGAAACTGTCTCC3′
Human renin	5′GCTATTCAACAGGGACAGTCAG3′/5′TCCGTGACCTCTCCAAACATC3′ 5′AGCCAGGACATCATCACCGTGGGT3′
Human ACE	5′TGCACAGTCTCAACCTGCTG3′/5′CAAGGGCCATCTTCATCAGAAAG3′ 5′TCAGCAGCTCCTAGTTCTTATGCCTTTGGT3′
Human AT1R	5′GGGGCGCGGGTGTATTTG3′/5′TTCAGTAGAAGAGTTGAGAATCATTTTG3′ 5′AGTGTTTGCAACAAATTCGACCCAGGTGA3′
Human AT2R	5′GCTGATTTATGATAACTGCTTTAAACTTC3′/5′GGTGGAGTTGCCCTTCATATTG3′ 5′TCAGCAGCTCCTAGTTCTTATGCCTTTGGT3′
Human adiponectin	5′CCGTGATGGCAGAGATGGCA3′/5′TGAGAAGGGTGAGAAAGGAGATCCAGGT3′ 5′CCGATGTCTCCCTTAGGACCAAT3′
Mice AGT	5′ACACCTACGTTCACTTCCAAG3′/5′CCGAGATGCTGTTGTCCAC3′ 5′ATGAGAGGTTTCTCTCAGCTGCCTGGA3′
Mice renin	5′GCTCCCTGAAGTTGATCATGC3′/5′GTGGGCACCTGGCTACAG3′ 5′CTCTTCTCCTTGGCTCCCAGGGCT3′
Mice ACE	5′TCCCAAAGTATGTGGAGTTCTCC3′/5′TTGTCAGACTCGTATAAGGATCTCC3′ 5′CCCTGCATCCGTGTAGCCATTGAGC3′
Mice AT1aR	5′TACCAGCTCTGCGGCTCTC3′/5′TGCTGTGAGTTATCCAGACAAAATG3′ 5′AGCTCTGCTGCTCTCCGGACTTAAC3′
Mice AT2R	5′GATGGAGGGAGCTCGGAAC3′/5′TTTAAAGCAGTTATCATAAATCAGCTTAC3′ 5′CACTCCTTAAAATGCAGGCTGAAGTAAGCT3′

The sequences of primers and probes for each gene used in this study are summarized.
AGT, angiotensinogen; ACE, angiotensin-converting enzyme; AT1R, angiotensin II type 1 receptor; AT1aR, angiotensin II type 1a receptor; AT2R, angiotensin II type 2 receptor.

buffer containing protease inhibitors (Complete; Roche, Basel, Switzerland).

Measurement of adipocyte diameter by a Coulter Multisizer. A total of 15 human subjects (5 men and 10 women; age: 51 ± 3.8 years; BMI: 28 ± 2.5 kg/m^2) were analyzed. Stromal-vascular cells and mature adipocytes (MAs) were isolated.[16] Adipocyte size was determined by a Beckman Coulter Multisizer III (Beckman Coulter, High Wycombe, UK).[12] Approximately 8,000 cells were analyzed using a Coulter Multisizer equipped with a 560-μm aperture tube. After collection of pulse sizes, data were expressed as particle diameters and displayed as histograms of counts against diameter, using linear bins and a linear scale for the *x*-axis.[12]

Statistical analyses. Values are expressed as mean ± s.e.m. Values not distributed normally were transformed into a logarithmic (natural logarithm) distribution and were analyzed using Pearson's correlation coefficient. A Student's *t*-test was used to compare the data (Social Research Information, Tokyo, Japan).

RESULTS

AGT mRNA expression and protein synthesis in 3T3–L1 adipocytes and human adipose tissue

Level of mRNA and protein of AGT were measured in lysates and cultured media in 3T3–L1 adipocytes treated with 10^{-9}, 10^{-8}, or 10^{-7} mol/l dexamethasone for 24 h. AGT protein level in lysates and cultured media were strongly correlated with the AGT mRNA level ($r = 0.98$, $P < 0.01$) (see **Supplementary Figure S3a** online) ($r = 0.84$, $P < 0.01$) (see **Supplementary Figure S3b** online).

Relationship between AGT protein/g adipose tissue and AGT mRNA levels in human SAT was also explored ($n = 7$, BMI: 29 ± 0.4 kg/m^2, range 19–48). Consistent with the results in 3T3–L1 adipocytes, AGT protein/g adipose tissue was correlated with the AGT mRNA level in human adipose tissue ($r = 0.77$, $P = 0.04$) (see **Supplementary Figure S3c** online).

Impact of adipose tissue–derived AGT secretion on obesity and blood pressure in humans

The mRNA levels of RAS genes, AGT, renin, ACE, AT1R, and AT2R in human SAT were analyzed. The AGT mRNA level was inversely correlated with BMI ($r = -0.32$, $P = 0.02$) (**Figure 1a**). On the other hand, no correlation was observed between the ACE mRNA level and BMI ($r = 0.08$, $P = 0.63$). The AT1R mRNA level was inversely correlated with BMI ($r = -0.32$, $P = 0.02$). Renin and AT2R mRNA levels were undetectable. The mRNA level of adiponectin was analyzed. No significant correlations were observed between adiponectin mRNA level and BMI ($r = 0.08$, $P = 0.56$) or AGT mRNA level ($r = 0.09$, $P = 0.49$). We also focused our attention on the possibilities of gender differences in AGT gene expression. When divided into two groups (BMI >25 (obese) and BMI <25 (lean)), the differences of AGT mRNA levels by gender were not observed in lean (male $n = 9$:female $n = 12$) and obese (male $n = 15$: female $n = 10$).

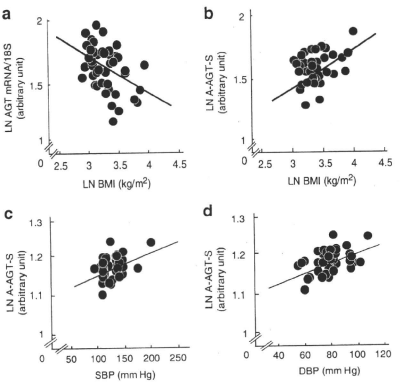

Figure 1 | Impact of adipose tissue–derived AGT secretion on obesity and blood pressure in humans. (**a**) Relation between AGT mRNA level and BMI ($n = 46$). (**b**) Relationship between adipose tissue–derived AGT secretion (A-AGT-S) and BMI ($n = 39$). (**c**) Relationship between A-AGT-S and systolic blood pressure (SBP) ($n = 39$). (**d**) Relationship between A-AGT-S and diastolic blood pressure (DBP) ($n = 39$). AGT, angiotensinogen; BMI, body mass index; LN, natural logarithm.

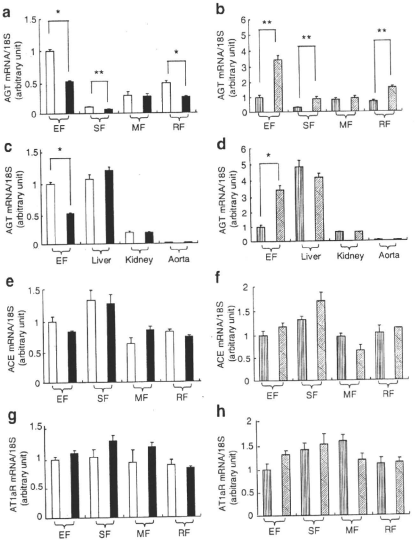

Figure 2 | Expression of genes involved in renin–angiotensin system in obese and weight-losing mouse. AGT mRNA levels in (**a**) 12W RD ($n = 6$) and 12W DIO ($n = 6$) and in (**b**) 14W DIO ($n = 6$) and 14W WL ($n = 6$) in epididymal fat (EF), subcutaneous fat (SF), mesenteric fat (MF), and retroperitoneal fat (RF). AGT mRNA levels in (**c**) 12W RD and 12W DIO and in (**d**) 14W DIO and 14W WL in the liver, kidney, and aorta. ACE mRNA levels in (**e**) 12W RD and 12W DIO and in (**f**) 14W DIO and 14W WL. AT1aR mRNA levels in (**g**) 12W RD and 12W DIO and in (**h**) 14W DIO and 14W WL. White bar, 12W RD; black bar, 12W DIO; vertical striping bar, 14W DIO; diagonal striping bar, 14W WL. *$P < 0.01$, **$P < 0.05$. ACE, angiotensin-converting enzyme; AGT, angiotensinogen; AT1aR, angiotensin II type 1a receptor; DIO, diet-induced obesity; WL, weight-losing.

Based on the results that AGT is secreted constitutively (see **Supplementary Figure S3a–c** online), AGT mRNA expression was predicted to parallel the AGT secretion. In this context, the amount of A-AGT-S was estimated by multiplying the mRNA level of AGT/g adipose tissue with serum leptin, a representative index of body fat mass. The serum leptin level in 55 subjects was correlated with body fat mass ($r = 0.76$, $P = 0.00000000001$). Contrary to AGT mRNA level, A-AGT-S was correlated with BMI ($n = 39$, $r = 0.36$, $P = 0.02$) (**Figure 1b**). A-AGT-S was correlated with systolic blood pressure ($n = 39$, $r = 0.36$, $P = 0.02$) (**Figure 1c**) and diastolic blood pressure ($n = 39$, $r = 0.45$, $P < 0.01$) (**Figure. 1d**). In both male group ($n = 20$) and female group ($n = 19$), A-AGT-S was correlated with BMI, systolic blood pressure, and diastolic blood pressure (data not shown).

Expression of genes involved in the RAS in obese and weight-losing mouse models

The mRNA levels of RAS genes were analyzed in obese and weight-losing mouse models described in Methods. The AGT mRNA levels in epididymal fat (EF), subcutaneous fat (SF), and retroperitoneal fat (RF) were lower in 12W DIO than in 12W RD (**Figure 2a**). In contrast, the AGT mRNA levels in EF, SF, and RF were elevated in 14W WL (**Figure 2b**). In the liver, kidney, and aorta, all of which are recognized as AGT-producing organs,[2] the AGT mRNA levels were equivalent between 12W DIO and 12W RD, or between 14W WL and 14W DIO (**Figure 2c,d**). Levels of ACE and angiotensin II type 1a receptor (AT1aR) mRNA in EF, SF, mesenteric fat (MF), and RF were also equivalent between 12W DIO and 12W RD or between 14W WL and 14W DIO (ACE: **Figure 2e,f**) (AT1aR: **Figure 2g,h**). AGT was decreased, although other genes involving RAS did not vary, in adipose tissue from the genetically obese *ob/ob* mice (data not shown).

Adipose tissue–derived AGT secretion and plasma AGT levels in obese and weight-losing mouse models

To assess the secretion of AGT from adipose tissue in body weight change, the amounts of A-AGT-S in obese and weight-losing mice were estimated by multiplying the AGT mRNA level/g adipose tissue with the weight of EF, SF, MF, or RF. The weights of EF, SF, MF, and RF in 12W DIO were increased ~3.5-fold in comparison with 12W RD, whereas the weights of EF, SF, MF, and RF in 14W WL were decreased by one-third compared to 14W DIO. Under caloric intervention, changes in weights in the liver and kidney were subtle compared to fat depots (~20% in liver and ~5% in kidney). A-AGT-S in EF, SF, MF, and RF was significantly increased

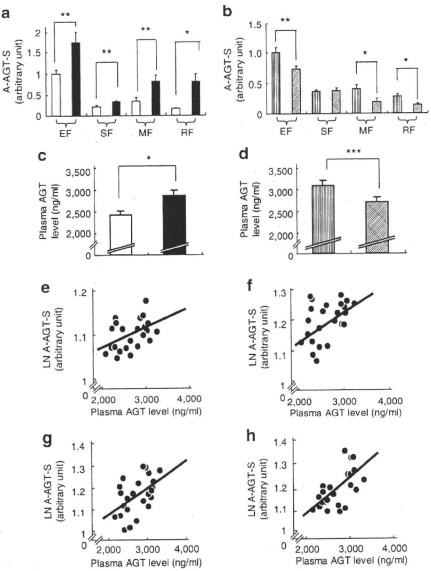

Figure 3 | Adipose tissue–derived AGT secretion and plasma AGT level between obese and weight-losing mouse. Adipose tissue–derived AGT secretion (A-AGT-S) in (**a**) 12W RD ($n = 6$) and 12W DIO ($n = 6$) and in (**b**) 14W DIO ($n = 6$) and 14W WL ($n = 6$) in epididymal fat (EF), subcutaneous fat (SF), mesenteric fat (MF), and retroperitoneal fat (RF). Plasma AGT levels in (**c**) 12W RD and 12W DIO and in (**d**) 14W DIO and 14W WL. Relationship between A-AGT-S and plasma AGT levels in (**e**) EF, (**f**) SF, (**g**) MF, and (**h**) RF. White bar, 12W RD; black bar, 12W DIO; vertical striping bar, 14W DIO; diagonal striping bar, 14W WL. *$P < 0.01$, **$P < 0.05$, ***$P = 0.05$. AGT, angiotensinogen; DIO, diet-induced obesity; LN, natural logarithm; WL, weight-losing.

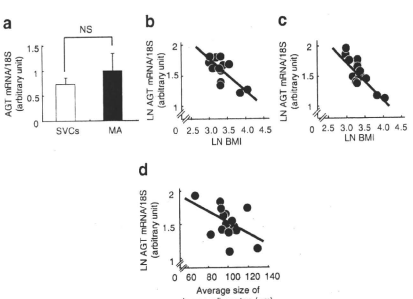

Figure 4 | Relationship between cell size and AGT mRNA level in isolated mature adipocytes in humans. (**a**) AGT mRNA level in stromal-vascular cells (SVCs) and mature adipocytes (MAs) isolated from human subcutaneous abdominal adipose tissue (SAT) ($n = 15$; BMI: 28 ± 2.5 kg/m^2). White bar, SVCs; black bar, MAs. Relationship between BMI and the AGT mRNA level in (**b**) SVCs or (**c**) MAs isolated from human SAT. (**d**) Relationship between the AGT mRNA level in MAs and the average size of large adipocytes in human SAT ($n = 15$; BMI: 28 ± 2.5 kg/m^2). AGT, angiotensinogen; LN, natural logarithm.

in 12W DIO compared to 12W RD (**Figure 3a**). In contrast, A-AGT-S in EF, MF, and RF was decreased in 14W WL compared to 14W DIO (**Figure 3b**). To further explore the impact of obesity on circulating AGT, plasma AGT levels were measured in 12W DIO, 12W RD, 14W WL, and 14W DIO using a newly developed ELISA.[10] The plasma AGT level was elevated in 12W DIO (2,884 ± 118 ng/ml) compared to 12W RD (2,431 ± 85 ng/ml) (**Figure 3c**). In contrast, the plasma AGT level in 14W WL (2,703 ± 116 ng/ml) was lower than in 14W DIO (3,088 ± 133 ng/ml) (**Figure 3d**). A-AGT-S in EF, SF, MF, and RF were correlated with plasma AGT level in mouse of obesity and weight reduction (EF: $r = 0.49$, $P < 0.01$ (**Figure 3e**); SF: $r = 0.43$, $P = 0.02$ (**Figure 3f**); MF: $r = 0.41$, $P = 0.03$ (**Figure 3g**); RF: $r = 0.64$, $P < 0.01$ (**Figure 3h**)).

Relationship between cell size and AGT mRNA level in isolated mature adipocytes in humans

To investigate the potential link between adipocyte size and the mRNA level of AGT in isolated MAs, adipocyte size was measured using a Coulter Multisizer[12] in human SAT ($n = 15$; BMI: 28 ± 2.5 kg/m^2, range: 19–55). The AGT mRNA level in MAs was comparable to that in stromal-vascular cells (**Figure 4a**).

The levels of AGT in stromal-vascular cells and MAs were inversely correlated with BMI ($r = -0.69$, $P < 0.01$ (**Figure 4b**), $r = -0.84$, $P < 0.01$ (**Figure 4c**). Consistent with a previous report,[12] the size distribution of adipocytes displayed as histograms against diameters was bimodal in all cases. The nadir was defined as the low point between the large adipocytes and small adipocytes.[12] BMI was positively correlated with both nadir size and average size of the larger adipocytes ($r = 0.50$, $P < 0.05$; $r = 0.48$, $P < 0.05$, respectively). The AGT mRNA level in isolated MA was inversely correlated with the average size of the larger adipocytes ($r = -0.48$, $P < 0.05$ (**Figure 4d**).

DISCUSSION

The primary findings of this study are (i) A-AGT-S was substantially increased in both obese humans and obese mice. (ii) A-AGT-S was correlated with plasma AGT level in mouse models of obesity and weight reduction. A-AGT-S and plasma AGT were increased in obese mice, while decreased in mice with weight reduction. (iii) The AGT mRNA level in adipose tissue was decreased in both obese humans and mice, but increased in mice with weight reduction. The AGT mRNA levels in the liver, kidney, and aorta were not altered in mouse models of obesity and weight reduction. In contrast, expression of genes involved in RAS other than AGT did not change in adipose tissue from obese and weight-losing mice. (iv) AGT was secreted constitutively from adipocytes and adipose tissue in both humans and mice. (v) Coulter Multisizer analyses revealed that the AGT mRNA level in MAs was correlated inversely with the average size of adipocytes larger than the nadir of bimodal histograms.

As AGT is secreted from many organs including liver, kidney, and vascular cells,[1,2] contribution of adipose tissue to plasma AGT level has not been determined. Furthermore, precise measurements of plasma AGT level were not conducted; instead, the radioimmunoassay result for angiotensin I has long been used as an equivalent.[1,17] In this context, an accurate assessment of A-AGT-S is critical for investigating clinical implications of adipose tissue RAS. Using a newly developed ELISA.[9,10] this study demonstrated for the first time that AGT was secreted constitutively from adipocytes and adipose tissue (**Supplementary Figures S3** online). Based on our novel finding, A-AGT-S was estimated by multiplying the mRNA level of AGT/g adipose tissue and fat mass or serum leptin, where applicable. Notably, only AGT is nutritionally regulated in adipose tissue from mice among RAS components (**Figure 2a,b,e–h**) reinforcing the rationale for focusing on A-AGT-S.

In this study, plasma AGT levels were increased ~20% in the obese mouse, whereas they were decreased ~12% in mice with weight reduction. A-AGT-S in EF, SF, MF, and RF was correlated with plasma AGT (**Figure 3e–h**). In contrast, AGT mRNA levels in the liver, kidney, and aorta were not altered in body weight changes (**Figure 2c,d**), suggesting adipose tissue–specific regulation of AGT in obesity. Under caloric intervention, changes in weights in the liver and kidney were subtle compared to fat depots, supporting the notion that AGT from the liver and kidney may not vary considerably in obesity or weight reduction. Taken together, it is reasonable to speculate that A-AGT-S contributes considerably (~20%) to plasma AGT level, accompanied by an increase in body fat mass.

Nevertheless the notion that visceral fat contributes to only ~10% of total adipose tissue mass in nonobese humans,[18] visceral adipose tissue–derived AGT secretion would not be negligible. In this context, in mouse models, we analyzed A-AGT-S in EF, MF, and RF, in addition to SF. A-AGT-S in EF, MF, and RF was increased in obese mice, whereas decreased in mice with weight reduction, and the A-AGT-S value in each adipose depot was correlated with plasma AGT level. Based on these results, it is likely to speculate that visceral adipose tissue–derived AGT secretion, like subcutaneous adipose tissue–derived AGT secretion, is substantially augmented and contributes to the plasma AGT level in human obesity.

Adipose tissue AGT mRNA levels were decreased by obesity and increased by weight loss, whereas A-AGT-S showed the opposite trend (**Figures 1–3**). It is likely that increased mass of adipose tissue in obesity overwhelmed the decrease in AGT expression, resulting in an increase in A-AGT-S and plasma AGT. Increased leptin mRNA level contributes to the extreme elevation of plasma leptin level in obesity.[19] Distinct from leptin, it is reasonable to speculate that AGT mRNA in adipose tissue is regulated so that plasma AGT concentration does not rise extremely in obesity. Although a series of hormonal and inflammatory changes may control AGT expression in adipose tissue,[1,20] the mechanism whereby AGT mRNA level is decreased exclusively in obese adipose tissue still remains obscure.

The mechanistic link between adipocyte size and metabolic consequences has long stimulated great interest in research.[11,12] To date, most of studies have employed histological analyses for assessing adipocyte size.[8,11] However, it should be noted that the distribution of adipocyte diameter is bimodal in humans.[12,13] Therefore, in this study, adipocyte size was analyzed using a Coulter Multisizer, which allows determination of the distribution of adipocyte size with greatest accuracy.[12] The progression of obesity is tightly associated with adipocyte hypertrophy.[21] In agreement with this notion, the average size of adipocytes larger than the nadir[12] was correlated with BMI ($r = 0.51$, $P = 0.03$), indicating that an increase in the average size of larger adipocytes tightly reflects adipocyte hypertrophy. The AGT mRNA level in isolated MAs was inversely correlated with the average size of larger adipocytes in humans (**Figure 4d**). We recently found that the AGT mRNA level was decreased in a long-term culture (~28 days) of 3T3-L1 adipocytes, with a concomitant increase in cellular triglyceride content (S. Okada, C. Kozuka, H. Masuzaki, S. Yasue, T. Ishii-Yonemato, Y. Yamamoto, M. Noguchi, T. Kusakabe, T. Tomita, J. Fujikura, K. Ebihara, K. Hosoda, H. Sakaue, H. Kobori, M. Ham, Y. Sok Lee, J. Bum Kim, Y. Saito, and K. Nakao, unpublished data). Although further studies are warranted, triglyceride accumulation and adipocyte hypertrophy may contribute to a decrease in AGT mRNA expression in obese adipose tissue.

In summary, this study is the first to demonstrate that secretion of adipose tissue–derived AGT is substantially augmented and contributes to the plasma AGT level in both obese humans and obese mice. Our results suggest that increase in adipose tissue–derived AGT contributes to circulating AGT level and resultant pathophysiology of obesity-related metabolic diseases.

Supplementary material is linked to the online version of the paper at http://www.nature.com/ajh

Acknowledgments: We are grateful to Mrs A. Ryu, S. Maki, and Ms. M. Nagamoto for assistance. This work was supported in part by a Grant-in-Aid for Scientific Research (B2), Takeda Medical Research Foundation, and Lilly Research Foundation. Clinical Trial Registration Number: UMIN000001969.

Disclosure: The authors declared no conflict of interest.

1. Engeli S, Schling P, Gorzelniak K, Boschmann M, Janke J, Ailhaud G, Teboul M, Massiéra F, Sharma AM. The adipose-tissue renin-angiotensin-aldosterone system: role in the metabolic syndrome? *Int J Biochem Cell Biol* 2002; 35: 807–825.
2. Dzau VJ. Circulating versus local renin-angiotensin system in cardiovascular homeostasis. *Circulation* 1988; 77:4–13.
3. Kurtz TW. Beyond the classic angiotensin-receptor-blocker profile. *Nat Clin Pract Cardiovasc Med* 2008; 5 Suppl 1:S19–S26.
4. Yusuf S, Sleight P, Pogue J, Bosch J, Davies R, Dagenais G. Effects of an angiotensin-converting-enzyme inhibitor, ramipril, on cardiovascular events in high-risk patients. The Heart Outcomes Prevention Evaluation Study Investigators. *N Engl J Med* 2000; 20:145–153.
5. Ogihara T, Nakao K, Fukui T, Fukiyama K, Saruta T. Clinical outcomes in hypertensive patients with high cardiovascular risks: principal results of candesartan antihypertensive survival evaluation in Japan (CASE-J) study. In: The 21st Scientific Meeting of the International Society of Hypertension, Fukuoka, Japan, 2006.
6. Massiera F, Bloch-Faure M, Ceiler D, Murakami K, Fukamizu A, Gasc JM, Quignard-Boulange A, Negrel R, Ailhaud G, Seydoux J, Meneton P, Teboul M. Adipose angiotensinogen is involved in adipose tissue growth and blood pressure regulation. *FASEB J* 2001; 15:2727–2729.
7. Giacchetti G, Faloia E, Mariniello B, Sardu C, Gatti C, Camilloni MA, Guerrieri M, Mantero F. Overexpression of the renin-angiotensin system in human visceral adipose tissue in normal and overweight subjects. *Am J Hypertens* 2002; 15:381–388.
8. Hainault I, Nebout G, Turban S, Ardouin B, Ferre P, Quignard-Boulange A. Adipose tissue-specific increase in angiotensinogen expression and secretion in the obese (fa/fa) Zucker rat. *Am J Physiol Endocrinol Metab* 2002; 282:E59–E66.
9. Katsurada A, Hagiwara Y, Miyashita K, Satou R, Miyata K, Ohashi N, Navar LG, Kobori H. Novel sandwich ELISA for human angiotensinogen. *Am J Physiol Renal Physiol* 2007; 293:F956–F960.
10. Kobori H, Katsurada A, Miyata K, Ohashi N, Satou R, Saito T, Hagiwara Y, Miyashita K, Navar LG. Determination of plasma and urinary angiotensinogen levels in rodents by newly developed ELISA. *Am J Physiol Renal Physio* 2008; 294: F1257–F1263.
11. Jernås M, Palming J, Sjöholm K, Jennische E, Svensson PA, Gabrielsson BG, Levin M, Sjögren A, Rudemo M, Lystig TC, Carlsson B, Carlsson LM, Lönn M. Separation of human adipocytes by size: hypertrophic fat cells display distinct gene expression. *FASEB J* 2006; 20:1540–1542.
12. McLaughlin T, Sherman A, Tsao P, Gonzalez O, Yee G, Lamendola C, Reaven GM, Cushman SW. Enhanced proportion of small adipose cells in insulin-resistant vs insulin-sensitive obese individuals implicates impaired adipogenesis. *Diabetologia* 2007; 50:1707–1715.
13. Julien P, Despres JP, Angel A. Scanning electron microscopy of very small fat cells and mature fat cells in human obesity. *J Lipid Res* 1989; 30:293–299.
14. Arai N, Masuzaki H, Tanaka T, Ishii T, Yasue S, Kobayashi N, Tomita T, Noguchi M, Kusakabe T, Fujikura J, Ebihara K, Hirata M, Hosoda K, Hayashi T, Sawai H, Minokoshi Y, Nakao K. Ceramide and adenosine 5′-monophosphate-activated protein kinase are two novel regulators of 11β-hydroxysteroid dehydrogenase type 1 expression and activity in cultured preadipocytes. *Endocrinology* 2007; 148:5268–5277.
15. Friedman JM, Halaas JL. Leptin and the regulation of body weight in mammals. *Nature* 1998; 395:763–770
16. Masuzaki H, Ogawa Y, Isse N, Satoh N, Okazaki T, Shigemoto M, Mori K, Tamura N, Hosoda K, Yoshimasa Y, Jingami H, Kawada T, Nakao K. Human obese gene expression. Adipocyte-specific expression and regional differences in the adipose tissue. *Diabetes* 1995; 44:855–858.
17. Umemura S, Nyui N, Tamura K, Hibi K, Yamaguchi S, Nakamaru M, Ishigami T, Yabana M, Kihara M, Inoue S, Ishii M. Plasma angiotensinogen concentrations in obese patients. *Am J Hypertens* 1997; 10:629–633.
18. Wajchenberg BL. Subcutaneous and visceral adipose tissue: their relation to the metabolic syndrome. *Endocr Rev* 2000; 21:697–738
19. Lönnqvist F, Nordfors L, Jansson M, Thörne A, Schalling M, Arner P. Leptin secretion from adipose tissue in women. Relationship to plasma levels and gene expression. *J Clin Invest* 1997; 99:2398–2404.
20. Aubert J, Darimont C, Safonova I, Ailhaud G, Negrel R. Regulation by glucocorticoids of angiotensinogen gene expression and secretion in adipose cells. *Biochem J* 1997; 328:701–706.
21. Bays HE, González-Campoy JM, Bray GA, Kitabchi AE, Bergman DA, Schorr AB, Rodbard HW, Henry RR. Pathogenic potential of adipose tissue and metabolic consequences of adipocyte hypertrophy and increased visceral adiposity. *Expert Rev Cardiovasc Ther* 2008; 6:343–368.

Diabetologia (2009) 52:675–683
DOI 10.1007/s00125-009-1258-2

ARTICLE

Beneficial effects of leptin on glycaemic and lipid control in a mouse model of type 2 diabetes with increased adiposity induced by streptozotocin and a high-fat diet

T. Kusakabe · H. Tanioka · K. Ebihara · M. Hirata · L. Miyamoto · F. Miyanaga · H. Hige · D. Aotani · T. Fujisawa · H. Masuzaki · K. Hosoda · K. Nakao

Received: 10 December 2008 / Accepted: 18 December 2008 / Published online: 24 January 2009

Abstract

Aims/hypothesis We have previously demonstrated the therapeutic usefulness of leptin in lipoatrophic diabetes and insulin-deficient diabetes in mouse models and could also demonstrate its dramatic effects on lipoatrophic diabetes in humans. The aim of the present study was to explore the therapeutic usefulness of leptin in a mouse model of type 2 diabetes with increased adiposity.

Methods To generate a mouse model mimicking human type 2 diabetes with increased adiposity, we used a combination of low-dose streptozotocin (STZ, 120 μg/g body weight) and high-fat diet (HFD, 45% of energy as fat). Recombinant mouse leptin was infused chronically (20 ng [g body weight]$^{-1}$ h^{-1}) for 14 days using a mini-osmotic pump. The effects of leptin on food intake, body weight, metabolic variables, tissue triacylglycerol content and AMP-activated protein kinase (AMPK) activity were examined.

Results Low-dose STZ injection led to a substantial reduction of plasma insulin levels and hyperglycaemia. Subsequent HFD feeding increased adiposity and induced insulin resistance and further augmentation of hyperglycaemia. In this model mouse mimicking human type 2 diabetes (STZ/HFD), continuous leptin infusion reduced food intake and body weight and improved glucose and lipid metabolism with enhancement of insulin sensitivity. Leptin also decreased liver and skeletal muscle triacylglycerol content accompanied by an increase of α2 AMPK activity in skeletal muscle. Pair-feeding experiments demonstrated that leptin improved glucose and lipid metabolism independently of the food intake reduction.

Conclusions/interpretation This study demonstrates the beneficial effects of leptin on glycaemic and lipid control in a mouse model of type 2 diabetes with increased adiposity, indicating the possible clinical usefulness of leptin as a new glucose-lowering drug in humans.

Keywords High-fat diet · Insulin sensitivity · Leptin · Overweight · Streptozotocin · Tissue triacylglycerol content · Type 2 diabetes

Abbreviations

AMPK	AMP-activated protein kinase
GTT	glucose tolerance test
HFD	high-fat diet
SD	standard diet
STZ	streptozotocin

Introduction

Leptin is an adipocyte-derived hormone that plays a key role in regulating food intake and energy expenditure, and participates in increasing glucose metabolism [1, 2]. Leptin deficiency causes obesity, insulin resistance and diabetes in mice and humans [3–5]. We previously generated transgenic skinny mice (LepTg) overexpressing leptin under the control of the liver-specific human serum amyloid P component promoter [6]. LepTg mice showed elevated

T. Kusakabe and H. Tanioka contributed equally to this work.

T. Kusakabe · H. Tanioka · K. Ebihara (✉) · M. Hirata · L. Miyamoto · F. Miyanaga · H. Hige · D. Aotani · T. Fujisawa · H. Masuzaki · K. Hosoda · K. Nakao
Department of Medicine and Clinical Science,
Kyoto University Graduate School of Medicine,
54 Shogoin Kawahara-cho,
Sakyo-ku, Kyoto 606-8507, Japan
e-mail: kebihara@kuhp.kyoto-u.ac.jp

plasma leptin levels comparable to those of obese human individuals, providing a unique experimental model to investigate various actions of leptin [6–11]. LepTg mice exhibited increased glucose metabolism and insulin sensitivity with augmented liver and skeletal muscle insulin receptor signalling [6]. LepTg mice also exhibited increased lipid metabolism accompanied by increased lipoprotein lipase activity and clearance of triacylglycerol [7]. In addition, LepTg mice had reduced tissue triacylglycerol content along with increased energy expenditure through augmented phosphorylation of AMP-activated protein kinase (AMPK), a key enzyme that mediates the leptin effect on fatty acid β-oxidation in skeletal muscle [8, 9]. Therefore, these findings led us to hypothesise that leptin acts as a glucose-lowering drug with a lipid-lowering effect in vivo.

Given the glucose-lowering action of leptin, we and others have demonstrated that leptin infusion or transgenic overexpression of leptin reverses metabolic abnormalities in different mouse models of lipodystrophy [10, 12]. Recently, we and others confirmed that leptin treatment effectively reduces food intake and improves hyperglycaemia, hypertriacylglycerolaemia and fatty liver in patients with lipoatrophic diabetes [13–16]. In addition, we demonstrated that leptin is useful as a glucose-lowering agent in a mouse model of insulin-deficient diabetes induced by high-dose streptozotocin (STZ) [11]. Leptin infusion reduced the dose of insulin required to improve hyperglycaemia by more than 90%, and prevented insulin-induced body weight gain in STZ-injected mice. However, the therapeutic usefulness of leptin in type 2 diabetes, a more prevalent form of diabetes, remains unclear.

In patients with type 2 diabetes, impaired insulin secretion caused by beta cell dysfunction and insulin resistance in target tissues contributes to increased blood glucose levels [17]. Patients with type 2 diabetes often exhibit dyslipidaemia and an increase of triacylglycerol content in the liver and skeletal muscle [18, 19]. Furthermore, in contrast to patients with lipoatrophic diabetes and insulin-deficient diabetes who are in hypoleptinaemic states [13–16, 20], patients with type 2 diabetes often have increased adiposity and elevated leptin levels.

Previous studies have shown that low-dose STZ injection leads to the partial destruction of pancreatic beta cells and a high-fat diet (HFD) induces insulin resistance in rodents [21–23]. The degree of beta cell destruction and insulin resistance can be adjusted by dosage, duration and condition of STZ injection and HFD feeding [11, 24]. The effects of various glucose-lowering drugs (sulfonylurea, metformin, thiazolidinedione etc) have been examined in mice treated with low-dose STZ and HFD as a model of type 2 diabetes [22, 23]. In the present study, we too generated a mouse model mimicking human type 2 diabetes using low-dose STZ and HFD to examine the effect of leptin infusion. STZ/HFD mice exhibited increased adiposity and disorders in glucose and lipid metabolism accompanied by impaired insulin secretion and insulin resistance. We report here the beneficial effects of leptin infusion on glycaemic and lipid control in this mouse model of type 2 diabetes with increased adiposity.

Methods

Animals Seven-week-old male C57BL/6J mice were purchased from Japan SLC, Shizuoka, Japan. The mice were caged individually and kept under a 12 h light–dark cycle (light on at 09:00 hours) with free access to water and standard diet (SD) (NMF, 14.6 kJ/g, 13% of energy as fat; Oriental Yeast Co., Tokyo, Japan) unless otherwise stated. Animal care and all experiments were conducted in accordance with the Guidelines for Animal Experiments of Kyoto University and were approved by the Animal Research Committee, Graduate School of Medicine, Kyoto University.

Generation of a mouse model of type 2 diabetes One week after purchase, mice were injected i.p. once with vehicle or low-dose STZ (120 μg/g body weight in 10 mmol/l sodium citrate buffer, pH 4.0; Sigma-Aldrich, St Louis, MO, USA) after 4 h of fasting. After 3 weeks, the vehicle-injected mice were randomly divided and placed on SD or HFD (D12451, 19.7 kJ/g, 45% of energy as fat; Research Diets, New Brunswick, NJ, USA) (termed control and HFD mice, respectively), and the STZ-injected mice with similar degrees of hyperglycaemia and body weight were also randomly divided and placed on SD or HFD (termed STZ and STZ/HFD mice, respectively). Each group of mice was fed with either diet for 5 weeks before they were used for the leptin infusion experiment.

Leptin infusion experiments On day 0, a mini-osmotic pump (Alzet model 2002; Alza, Palo Alto, CA, USA) was implanted s.c. in the mid-scapular region of each mouse. The pump delivered saline or recombinant mouse leptin (Amgen, Thousand Oaks, CA, USA) (20 ng [g body weight]$^{-1}$ h^{-1}) s.c. for 14 days. SD or HFD feeding was continued during the leptin infusion experiment.

Food intake, body weight and per cent body fat Food intake was measured before and during the leptin infusion experiment. Body weight was measured on days 0 and 14. Per cent body fat was measured before the leptin infusion experiment under pentobarbital anaesthesia (Nembutal; Dainippon Sumitomo Pharma, Osaka, Japan), using a Latheta LTC-100 (Aloka, Tokyo, Japan).

Metabolic variables Blood was obtained from non-fasted mice between 15:00 and 17:00 hours. Blood glucose levels were determined by the glucose oxidase method using a reflectance glucometer (MS-GR102; Terumo, Tokyo, Japan) on days 0, 4, 7 and 14. Plasma insulin levels were measured by enzyme immunoassay with an Insulin-EIA kit (Morinaga, Tokyo, Japan). Plasma triacylglycerol, NEFA and total cholesterol levels were measured using enzymatic kits (Triglyceride E-test Wako, NEFA C-test Wako and Cholesterol E-test Wako, respectively; Wako Pure Chemicals, Osaka, Japan). Plasma leptin levels were determined using an RIA kit for mouse leptin (Linco Research Immunoassay, St Louis, MO, USA).

Glucose tolerance test (GTT) A GTT was performed on day 10. Mice were injected i.p. with 2.0 mg/g glucose after overnight fasting. Blood glucose and plasma insulin levels were measured at the indicated time points.

Liver and skeletal muscle triacylglycerol content Tissue triacylglycerol content was measured as described previously [7, 8], with modifications. Liver and quadriceps muscle were isolated at the end of the leptin infusion experiment, immediately frozen in liquid nitrogen and lipids extracted with isopropyl alcohol/heptane (1:1 vol./vol.). After evaporating the solvent, the lipids were resuspended in 99.5% (vol./vol.) ethanol, and the triacylglycerol content was measured using the Triglyceride E-test Wako kit.

Isoform-specific AMPK activity AMPK activity was determined as described previously [25, 26], with modifications. To measure α1 and α2 isoform-specific AMPK activity in skeletal muscle, AMPK was immunoprecipitated from muscle lysates (200 μg protein) with specific antibodies against the α1- and α2-subunits (Upstate Cell Signaling Solutions, Lake Placid, NY, USA) bound to Protein A-Sepharose beads, and the kinase activity of the immunoprecipitates was measured using 'SAMS' peptide and [γ-^{32}P]ATP.

Pair-feeding experiments STZ or STZ/HFD mice were fed the same amount of food consumed by the corresponding leptin-infused mice on the previous day, for 14 days. A GTT was performed on day 10 of the experiment. Liver and quadriceps muscle were obtained for triacylglycerol content measurements at the end of the pair-feeding experiment.

Statistical analyses Data are expressed as means±SEM. Comparison between or among groups was by Student's *t* test or ANOVA with Fisher's protected least significant difference test. $p<0.05$ was considered statistically significant.

Results

Generation of a mouse model of type 2 diabetes To generate a mouse model mimicking human type 2 diabetes with impaired insulin secretion and insulin resistance, we used low-dose STZ injection and HFD feeding. As shown in Table 1, HFD feeding effectively increased body weight, per cent body fat and plasma leptin levels in mice. With the development of adiposity, plasma insulin levels substan-

Table 1 Metabolic characteristics of the mouse model of type 2 diabetes

Variable	Mouse group			
	Control	HFD	STZ	STZ/HFD
Food intake (kJ/week)	329.0±9.3	350.7±20.0	365.3±15.1*	422.1±23.1**,†
Body weight (g)	26.8±0.6	34.4±1.3**	26.4±0.4	27.9±0.5†
Body fat (%)	19.8±0.7	40.6±1.1**	18.9±1.0	24.9±1.8*,†
Leptin (ng/ml)	4.7±0.6	26.4±1.0**	4.5±0.5	8.6±0.8**,††
Glucose (mmol/l)	8.3±0.2	9.2±0.4	17.5±2.3**	27.2±1.2**,††
Insulin (pmol/l)	160±28	315±71*	92±12*	160±38
Triacylglycerol (mmol/l)	0.66±0.09	0.86±0.08	1.11±0.14*	1.27±0.28*
NEFA (mEq/l)	0.77±0.06	1.08±0.09*	1.03±0.10*	0.99±0.09*
Total cholesterol (mmol/l)	1.48±0.08	3.61±0.18**	1.49±0.16	3.01±0.19**,††
Liver triacylglycerol content (mg/g tissue)	8.7±1.0	20.0±2.2**	10.2±0.9	27.1±1.7**,††
Skeletal muscle triacylglycerol content (mg/g tissue)	5.6±0.5	8.1±1.2*	5.4±0.5	7.8±0.8*,†

Values are means±SEM for 10–12 mice in each group
C57BL/6J mice were injected with vehicle and fed SD (control) or HFD, or injected with low-dose STZ and fed with SD (STZ) or HFD (STZ/HFD). Food intake for a week, body weight, per cent body fat, blood glucose levels and plasma levels for leptin, insulin, triacylglycerol, NEFA and total cholesterol were measured before the leptin infusion experiment. Blood samples were obtained during ad libitum feeding. Liver and skeletal muscle triacylglycerol contents were measured after the leptin infusion experiment
*$p<0.05$, **$p<0.01$ vs control mice; †$p<0.05$, ††$p<0.01$ vs STZ in STZ/HFD mice

tially increased, although blood glucose levels did not significantly increase, suggesting the development of insulin resistance. HFD feeding also increased plasma NEFA and total cholesterol levels, and liver and skeletal muscle triacylglycerol contents.

Low-dose STZ injection led to a substantial reduction of plasma insulin and hyperglycaemia in mice. Under these conditions, body weight, per cent body fat and plasma leptin levels were unchanged, although food intake was significantly increased. Low plasma insulin levels also led to an increase of plasma triacylglycerol and NEFA levels. Liver and skeletal muscle triacylglycerol contents were unchanged.

On the other hand, subsequent HFD feeding in low-dose STZ injected mice further increased food intake and moderately increased body weight, per cent body fat and plasma leptin levels even with the impairment of insulin secretion. Hyperglycaemia was exacerbated, although plasma insulin levels were mildly elevated, suggesting the development of insulin resistance. Increases of plasma triacylglycerol, NEFA and total cholesterol levels, and liver and skeletal muscle triacylglycerol contents, were also observed in these STZ/HFD mice.

Since STZ/HFD mice manifested increased adiposity and disorders in glucose and lipid metabolism accompanied by impaired insulin secretion and insulin resistance, we used STZ/HFD mice as a model of type 2 diabetes with increased adiposity in the present study.

Effect of leptin on food intake and body weight As shown in Fig. 1a, continuous leptin infusion elevated plasma leptin levels from baseline almost equally in control, HFD, STZ and STZ/HFD mice. Under these conditions, food intake was significantly suppressed in control, STZ and STZ/HFD mice, while that in HFD was unchanged (Fig. 1b). Consistent with food intake, body weight was effectively decreased in control, STZ and STZ/HFD mice, while that in HFD mice was unchanged (Fig. 1c).

Effect of leptin on glucose metabolism In control mice, leptin infusion did not affect blood glucose levels during ad libitum feeding but markedly decreased plasma insulin levels, suggesting the enhancement of insulin sensitivity (Fig. 2a, e). In HFD mice, leptin infusion showed no effect on either blood glucose levels or plasma insulin levels (Fig. 2b, e). On the other hand, both blood glucose levels and plasma insulin levels were effectively decreased after 2 weeks of leptin infusion in STZ and STZ/HFD mice, suggesting the improvement of insulin sensitivity (Fig. 2c–e).

To further evaluate the effect of leptin on glucose metabolism, we performed i.p. GTTs (Fig. 3). In control, STZ and STZ/HFD mice, leptin infusion significantly improved glucose tolerance with reduction of plasma insulin levels not only in the fasting state but also after the glucose load, suggesting an improvement of insulin sensitivity. In contrast, in HFD mice, leptin infusion did not improve glucose tolerance and also did not suppress plasma insulin levels before or after glucose load.

Effect of leptin on plasma lipid profiles Leptin infusion did not affect plasma triacylglycerol, NEFA and total cholesterol levels in control mice (Fig. 4a–c). Leptin infusion also did not change plasma triacylglycerol, NEFA and total cholesterol levels in HFD mice, even though basal plasma NEFA and total cholesterol levels were elevated. In STZ mice, leptin infusion effectively decreased plasma triacylglycerol and NEFA levels, which were elevated at baseline, while leptin infusion did not affect plasma total cholesterol levels, which were not elevated at baseline. In STZ/HFD

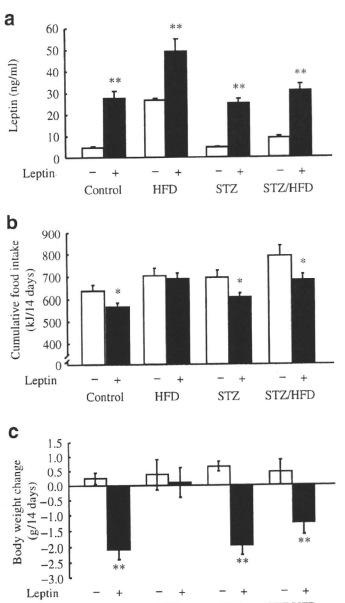

Fig. 1 Effect of leptin on leptin levels, food intake and body weight. Leptin levels on day 14 (**a**), cumulative food intake (**b**) and change in body weight (**c**) after 14 days of leptin infusion in control, HFD, STZ and STZ/HFD mice. Values are means±SEM (n=10–17). *p<0.05, **p<0.01 vs corresponding saline-infused mice

mice, leptin infusion also effectively decreased plasma triacylglycerol, NEFA and total cholesterol levels, which were elevated at baseline.

Effect of leptin on liver and skeletal muscle triacylglycerol contents To assess whether the improvement of glucose metabolism by leptin infusion was associated with the reduction of triacylglycerol content in insulin-target tissues, we examined the effect of leptin infusion on liver and skeletal muscle triacylglycerol contents. As shown in Fig. 5, leptin infusion apparently decreased triacylglycerol contents of both liver and skeletal muscle in control, STZ and STZ/HFD mice, in which glucose metabolism was improved by leptin infusion. In contrast, leptin infusion decreased triacylglycerol content of neither liver nor skeletal muscle in HFD mice, in which glucose metabolism was unchanged by leptin infusion.

Effect of leptin on AMPK activity in skeletal muscle Leptin infusion did not affect α1 isoform-specific AMPK activity in skeletal muscle in any group of mice (Fig. 6a). On the other hand, leptin infusion significantly increased α2 isoform-specific AMPK activity in skeletal muscle in control, STZ and STZ/HFD mice (Fig. 6b). However, no significant increase of α2 AMPK activity in skeletal muscle was observed in HFD mice.

Pair-feeding experiments We investigated whether the reduction of food intake by leptin infusion is the reason

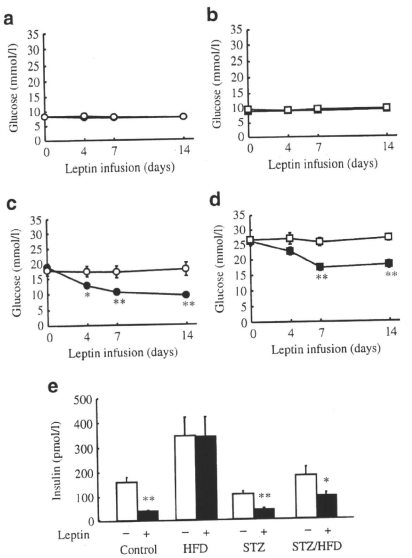

Fig. 2 Effect of leptin infusion for 14 days on blood glucose and plasma insulin levels during ad libitum feeding. Blood glucose levels on days 0, 4, 7 and 14 in control (**a**), HFD (**b**), STZ (**c**) and STZ/HFD mice (**d**). White symbols, saline-infused; black symbols, leptin-infused. **e** Plasma insulin levels during ad libitum feeding on day 14 in control, HFD, STZ and STZ/HFD mice. Values are means±SEM (n=10–17). *p<0.05, **p<0.01 vs corresponding saline-infused mice

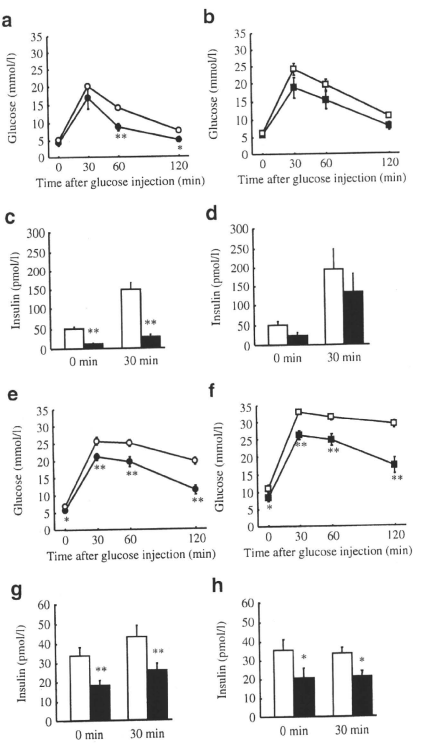

Fig. 3 Effect of leptin on glucose tolerance and insulin secretion during GTTs. Blood glucose and plasma insulin levels were measured at the indicated time points in control (**a**, **c**), HFD (**b**, **d**), STZ (**e**, **g**) and STZ/HFD mice (**f**, **h**). Values are means±SEM (n=10–17). *p<0.05, **p<0.01 vs corresponding saline-infused mice

for its efficacy in improving glucose metabolism. We pair-fed STZ and STZ/HFD mice the same amount of food consumed by the corresponding leptin-infused mice on the previous day. Pair-feeding did not improve glucose tolerance in GTTs in STZ and STZ/HFD mice (data not shown). Moreover, when compared with basal values (Table 1), no significant decrease of liver and skeletal muscle triacylglycerol contents was observed in pair-fed STZ and STZ/HFD mice (liver triacylglycerol content: 8.3±1.2 and 30.0±5.6 mg/g tissue; skeletal muscle triacylglycerol content: 5.4±0.5 and 6.6±0.5 mg/g tissue, in pair-fed STZ and STZ/HFD mice, respectively, n=5 in each group of mice), in contrast to the corresponding leptin-infused mice (Fig. 5).

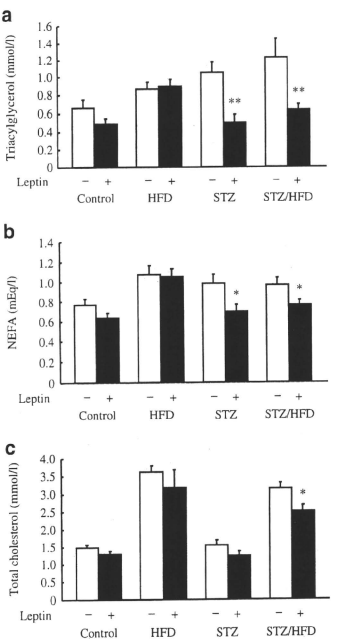

Fig. 4 Effect of leptin on plasma lipid profiles. Plasma triacylglycerol (**a**), NEFA (**b**) and total cholesterol levels (**c**) during ad libitum feeding on day 14 in control, HFD, STZ and STZ/HFD mice. Values are means±SEM (n=10–17). *p<0.05, **p<0.01 vs corresponding saline-infused mice

Discussion

The effectiveness of leptin treatment in diabetes has been reported in patients with leptin deficiency and lipodystrophy and in amenorrhoea in patients with hypothalamic hypogonadism caused by low body weight [5, 13–16, 27]. These patients are in hypoleptinaemic states, and hypoleptinaemia is involved in the pathophysiology of their diseases. However, whether leptin treatment is effective in normo- or hyperleptinaemic states has not been fully examined. The aim of the present study was to explore the therapeutic usefulness of leptin in type 2 diabetes, which is often accompanied by increased adiposity. Type 2 diabetes develops as a result of insulin resistance in target tissues and impaired insulin secretion, accompanied by increased adiposity. To generate a mouse model mimicking human type 2 diabetes, we used a combination of low-dose STZ and HFD. Although high-dose STZ injection generally reduces body weight, with a marked reduction of insulin levels [16], low-dose STZ used in this study did not reduce body weight. In addition, subsequent HFD feeding in low-dose STZ injected mice could increase body weight even

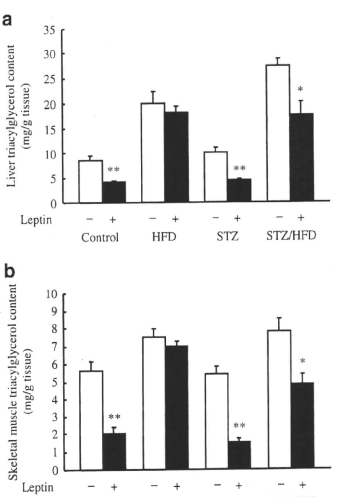

Fig. 5 Effect of leptin on liver and skeletal muscle triacylglycerol contents. Liver (**a**) and skeletal muscle (**b**) triacylglycerol contents on day 14 in STZ and STZ/HFD mice. Values are means±SEM (n=10–13). *p<0.05, **p<0.01 vs corresponding saline-infused mice

with the impairment of insulin secretion in this study. Consistent with the increase in body weight and per cent body fat, STZ/HFD mice showed a nearly twofold increase in plasma leptin levels compared with control mice (Table 1). In humans, plasma leptin levels positively correlated with BMI, and a twofold increase in plasma leptin levels corresponds to a BMI in the range of 25–30 kg/m^2 [28, 29]. According to recent clinical studies, the average BMI in patients with type 2 diabetes is within this overweight range [30–32]. HFD mice showed a larger increase in adiposity and plasma leptin levels than did STZ/HFD mice. However, unlike STZ/HFD mice, HFD mice did not develop hyperglycaemia, because of compensatory hyperinsulinaemia. Therefore, we used STZ/HFD mice as an appropriate model to examine the efficacy of leptin in type 2 diabetes with increased adiposity.

The present study showed that the effect of leptin on food intake and body weight was attenuated in obese HFD mice (Fig. 1b, c). In general, in human obesity and rodent models of diet-induced obesity, even though leptin levels rise proportionally with adiposity, the increased leptin fails to suppress the progression of obesity. Moreover, obese humans and rodents are weakly responsive to exogenously administered leptin in terms of body weight reduction [33, 34]. This leptin ineffectiveness is called leptin resistance. The present study also showed that the effect of leptin on glucose and lipid metabolism was attenuated in obese HFD mice (Figs 2, 3, 4 and 5). In contrast, even under HFD feeding, leptin effectively improved glucose and lipid metabolism in STZ/HFD mice. Impaired insulin secretion caused by STZ injection could reduce the effect of HFD feeding on the development of obesity in STZ/HFD mice. As a result, leptin resistance could be mild, if any, in STZ/HFD mice. The present study demonstrated that leptin could be a glucose-lowering drug for the treatment of type 2 diabetes with impaired insulin secretion.

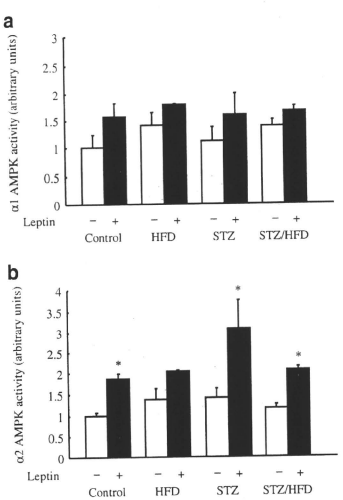

Fig. 6 Effect of leptin on isoform-specific AMPK activity in skeletal muscle. α1 AMPK activity (**a**) and α2 AMPK activity (**b**) on day 14 in soleus muscle of STZ and STZ/HFD mice. Values are means±SEM (n=4–5). *p<0.05 vs corresponding saline-infused mice

Fat accumulation in insulin target tissues is considered to be one of the causes of insulin resistance, and is called lipotoxicity [35, 36]. Indeed, HFD and STZ/HFD mice exhibited insulin resistance and increased liver and skeletal muscle triacylglycerol contents (Table 1). In the present study, we investigated an association between the improvement of glucose metabolism by leptin infusion and the reduction of liver and skeletal muscle triacylglycerol contents. Leptin infusion enhanced insulin sensitivity in control, STZ and STZ/HFD mice, in which it decreased liver and skeletal muscle triacylglycerol contents (Figs 3 and 5). In contrast, leptin infusion did not improve insulin resistance in HFD mice, in which it did not decrease liver and skeletal muscle triacylglycerol contents. Moreover, pair-feeding neither improved glucose tolerance nor decreased the liver and skeletal muscle triacylglycerol contents in STZ and STZ/HFD mice. These results suggest that the improvement of glucose metabolism by leptin infusion is associated with a reduction in liver and skeletal muscle triacylglycerol contents.

Leptin has been shown to selectively stimulate activation of the α2 catalytic subunit of AMPK in skeletal muscle [37]. AMPK is a key enzyme that mediates the leptin effect on fatty acid β-oxidation in skeletal muscle. In the present study, leptin infusion effectively decreased skeletal muscle triacylglycerol content in control, STZ and STZ/HFD mice (Fig. 5b), in which it increased α2 AMPK activity in skeletal muscle (Fig. 6b). In contrast, leptin infusion did not decrease skeletal muscle triacylglycerol content in HFD mice (Fig. 5b), in which it did not increase α2 AMPK activity in skeletal muscle (Fig. 6b). Increased fatty acid β-oxidation through α2 AMPK activation in skeletal muscle is considered to be one of the mechanisms by which leptin decreases skeletal muscle triacylglycerol content [9].

The present study also showed that leptin infusion effectively improved hyperlipidaemia in STZ and STZ/HFD mice (Fig. 4). Increased lipoprotein lipase activity, increased clearance of triacylglycerol [7], reduction of triacylglycerol synthesis by controlling key transcription factors [38] and increased energy expenditure through fatty acid β-oxidation have been reported as mechanisms by

which leptin decreases plasma triacylglycerol levels. The present study demonstrated activation of α2 AMPK activity by leptin infusion in skeletal muscle (Fig. 6b), which might contribute to increased energy expenditure in our leptin-infused STZ and STZ/HFD mice. It is also well known that impaired insulin action induces hyperlipidaemia [39]. It is also possible that leptin improved hyperlipidaemia by enhancement of insulin sensitivity in the present study.

The present study demonstrated that pair-feeding neither improved glucose tolerance nor decreased liver and skeletal muscle triacylglycerol contents in STZ and STZ/HFD mice. Previously, we and others have demonstrated that food intake reduction alone was insufficient for improving glucose and lipid metabolism [6, 10, 12]. It has also been reported that fasting insulin and triacylglycerol levels increased within several days after withdrawal of leptin administration even though the level of food intake remained constant in the patients with lipodystrophy [13]. Furthermore, it has been demonstrated that leptin administration decreases liver and skeletal muscle triacylglycerol contents in patients with lipodystrophy [40]. These results indicate that leptin improves glucose and lipid metabolism independently of the food intake reduction.

With the dose of leptin used in the present study, the plasma leptin levels in STZ/HFD mice increased to the levels of obese HFD mice (mean leptin levels in leptin-infused STZ/HFD mice, 30.8 ng/ml) (Fig. 1a), which can be seen in human obese individuals. In our clinical research on leptin-replacement therapy in patients with generalised lipodystrophy, the peak plasma leptin levels of the 400% dose under the protocol of once-daily injections was 34.5± 2.1 (mean±SE) ng/ml, and the therapy was well tolerated without any adverse effects for about 5 years [15]. In addition, higher leptin levels were obtained in the obese human clinical trial [33]. Therefore, the leptin levels achieved with the dose used in the present study could be clinically applied in humans.

In conclusion, the present study demonstrates that leptin therapy improves glucose and lipid metabolism and enhances insulin sensitivity in a mouse model of type 2 diabetes with an overweight range of adiposity. Our findings indicate that leptin could be a new glucose-lowering drug for the treatment of type 2 diabetes in humans.

Acknowledgements We thank M. Nagamoto for technical assistance and Y. Koyama for secretarial assistance. This work was supported in part by research grants from the Ministry of Education, Culture, Sports, Science and Technology of Japan; the Ministry of Health, Labour and Welfare of Japan; the Takeda Medical Research Foundation and Japan Foundation of Applied Enzymology; and the ONO Medical Research Foundation.

Duality of interest The authors declare that there is no duality of interest associated with this manuscript.

References

1. Halaas JL, Gajiwala KS, Maffei M (1995) Weight-reducing effects of the plasma protein encoded by the obese gene. Science 269:543–546
2. Friedman JM, Halaas JL (1998) Leptin and the regulation of body weight in mammals. Nature 395:763–770
3. Muzzin P, Eisensmith RC, Copeland KC, Woo SLC (1996) Correction of obesity and diabetes in genetically obese mice by leptin gene therapy. Proc Natl Acad Sci U S A 93:14804–14808
4. Montague CT, Farooqi IS, Whitehead JP (1997) Congenital leptin deficiency is associated with severe early-onset obesity in humans. Nature 387:903–908
5. Licinio J, Caglayan S, Ozata M (2004) Phenotypic effects of leptin replacement on morbid obesity, diabetes mellitus, hypogonadism, and behavior in leptin-deficient adults. Proc Natl Acad Sci U S A 101:4531–4536
6. Ogawa Y, Masuzaki H, Hosoda K (1999) Increased glucose metabolism and insulin sensitivity in transgenic skinny mice overexpressing leptin. Diabetes 48:1822–1829
7. Matsuoka N, Ogawa Y, Masuzaki H (2001) Decreased triglyceride-rich lipoproteins in transgenic skinny mice overexpressing leptin. Am J Physiol Endocrinol Metab 280:E334–E339
8. Tanaka T, Masuzaki H, Yasue S (2007) Central melanocortin signaling restores skeletal muscle AMP-activated protein kinase phosphorylation in mice fed a high-fat diet. Cell Metabolism 5:395–402
9. Tanaka T, Hidaka S, Masuzaki H (2005) Skeletal muscle AMP-activated protein kinase phosphorylation parallels metabolic phenotype in leptin transgenic mice under dietary modification. Diabetes 54:2365–2374
10. Ebihara K, Ogawa Y, Masuzaki H (2001) Transgenic overexpression of leptin rescues insulin resistance and diabetes in a mouse model of lipoatrophic diabetes. Diabetes 50:1440–1448
11. Miyanaga F, Ogawa Y, Ebihara K (2003) Leptin as an adjunct of insulin therapy in insulin-deficient diabetes. Diabetologia 46:1329–1337
12. Shimomura I, Hammer RE, Ikemoto S, Brown MS, Goldstein JL (1999) Leptin reverses insulin resistance and diabetes mellitus in mice with congenital lipodystrophy. Nature 401:73–76
13. Oral EA, Simha V, Ruiz E (2002) Leptin-replacement therapy for lipodystrophy. N Engl J Med 346:570–578
14. Ebihara K, Masuzaki H, Nakao K (2004) Long-term leptin-replacement therapy for lipoatrophic diabetes. N Engl J Med 351:615–616
15. Ebihara K, Kusakabe T, Hirata M (2007) Efficacy and safety of leptin-replacement therapy and possible mechanisms of leptin actions in patients with generalized lipodystrophy. J Clin Endocrinol Metab 92:532–541
16. Beltrand J, Beregszaszi M, Chevenne D (2007) Metabolic correction induced by leptin replacement treatment in young children with Berardinelli–Seip congenital lipoatrophy. Pediatrics 120:e291–e296
17. Taylor SI (1999) Deconstructing type 2 diabetes. Cell 97:9–12
18. Ishii M, Yoshioka Y, Ishida W (2005) Liver fat content measured by magnetic resonance spectroscopy at 3.0 tesla independently correlates with plasminogen activator inhibitor-1 and body mass index in type 2 diabetic subjects. Tohoku J Exp Med 206:23–30
19. Sinha R, Dufour S, Petersen KF (2002) Assessment of skeletal muscle triglyceride content by ^{1}H nuclear magnetic resonance spectroscopy in lean and obese adolescents: relationships to insulin sensitivity, total body fat, and central adiposity. Diabetes 51:1022–1027
20. Kiess W, Anil M, Blum WF (1998) Serum leptin levels in children and adolescents with insulin-dependent diabetes mellitus in relation to metabolic control and body mass index. Eur J Endocrinol 138:501–509

21. Ding SY, Shen ZF, Chen YT, Sun SJ, Liu Q, Xie MZ (2005) Pioglitazone can ameliorate insulin resistance in low-dose streptozotocin and high sucrose-fat diet induced obese rats. Acta Pharmacol Sin 26:575–580
22. Luo J, Quan J, Tsai J (1998) Nongenetic mouse models of non-insulin-dependent diabetes mellitus. Metabolism 47:663–668
23. Mu J, Woods J, Zhou YP (2006) Chronic inhibition of dipeptidyl peptidase-4 with a sitagliptin analog preserves pancreatic β-cell mass and function in a rodent model of type 2 diabetes. Diabetes 55:1695–1704
24. Shertzer HG, Schneider SN, Kendig EL, Clegg DJ, D'Alessio DA, Genter MB (2008) Acetaminophen normalizes glucose homeostasis in mouse models for diabetes. Biochem Pharmacol 75:1402–1410
25. Miyamoto L, Toyoda T, Hayashi T (2007) Effect of acute activation of 5′-AMP-activated protein kinase on glycogen regulation in isolated rat skeletal muscle. J Appl Physiol 102:1007–1013
26. Toyoda T, Tanaka S, Ebihara K (2006) Low-intensity contraction activates the alpha1-isoform of 5′-AMP-activated protein kinase in rat skeletal muscle. Am J Physiol Endocrinol Metab 290:E583–E590
27. Welt CK, Chan JL, Bullen J (2004) Recombinant human leptin in women with hypothalamic amenorrhea. N Engl J Med 351:987–997
28. Buettner R, Bollheimer LC, Zietz B (2002) Definition and characterization of relative hypo- and hyperleptinemia in a large Caucasian population. J Endocrinol 175:745–756
29. Peltz G, Sanderson M, Pérez A, Sexton K, Ochoa Casares D, Fadden MK (2007) Serum leptin concentration, adiposity, and body fat distribution in Mexican–Americans. Arch Med Res 38:563–570
30. Widjaja A, Stratton IM, Horn R, Holman RR, Tuner R, Brabant G (1997) UKPDS 20: Plasma leptin, obesity, and plasma insulin in type 2 diabetic subjects. J Clin Endocrinol Metab 82:654–657
31. Sone H, Yoshimura Y, Tanaka S (2007) Cross-sectional association between BMI, glycemic control and energy intake in Japanese patients with type 2 diabetes. Analysis from the Japan Diabetes Complications Study. Diabetes Res Clin Pract 77S:S23–S29
32. Sone H, Ito H, Ohashi Y, Akanuma Y, Yamada N, Japan Diabetes Complications Study (JDCS) Group (2003) Obesity and type 2 diabetes in Japanese patients. Lancet 361:85
33. Heymsfield SB, Greenberg AS, Fujioka K (1999) Recombinant leptin for weight loss in obese and lean adults: a randomized, controlled, dose-escalation trial. JAMA 282:1568–1575
34. El-Haschimi K, Pierroz DD, Hileman SM, Bjorbaek C, Flier JS (2000) Two defects contribute to hypothalamic leptin resistance in mice with diet-induced obesity. J Clin Invest 105:1827–1832
35. Schulman GI (2000) Cellular mechanisms of insulin resistance. J Clin Invest 106:171–176
36. Unger RH (2003) Minireview: Weapons of lean body mass destruction: the role of ectopic lipids in the metabolic syndrome. Endocrinology 144:5159–5165
37. Minokoshi Y, Kim YB, Peroni OD (2002) Leptin stimulates fatty-acid oxidation by activating AMP-activated protein kinase. Nature 415:339–343
38. Cohen P, Miyazaki M, Socci ND (2002) Role for stearoyl-CoA desaturase-1 in leptin-mediated weight loss. Science 297:240–243
39. Reaven GM (2005) Why Syndrome X? From Harold Himsworth to the insulin resistance syndrome. Cell Metab 1:9–14
40. Petersen KF, Oral EA, Dufour S (2002) Leptin reverses insulin resistance and hepatic steatosis in patients with severe lipodystrophy. J Clin Invest 109:1345–1350

0888-8809/08/$15.00/0
Printed in U.S.A.

Molecular Endocrinology 22(9):2176–2189

doi: 10.1210/me.2008-0023

Dysregulation of Adipose Glutathione Peroxidase 3 in Obesity Contributes to Local and Systemic Oxidative Stress

Yun Sok Lee, A Young Kim, Jin Woo Choi, Min Kim, Shintaro Yasue, Hee Jung Son, Hiroaki Masuzaki, Kyong Soo Park, and Jae Bum Kim

Institute of Molecular Biology and Genetics (Y.S.L., A.Y.K., J.W.C., J.B.K.) and Department of Biological Sciences, Research Center for Functional Cellulomics (Y.S.L., A.Y.K., J.W.C., J.B.K.), Seoul National University, Seoul 151-742, Korea; Department of Internal Medicine (M.K., K.S.P.), Seoul National University College of Medicine, Seoul 110-744, Korea; Department of Medicine and Clinical Science (S.Y., H.M.), Kyoto University Graduate School of Medicine, Kyoto 606-8507, Japan; and Samsung Medical Center (H.J.S.), Seoul 135-230, Korea

Glutathione peroxidase 3 (GPx3) accounts for the major antioxidant activity in the plasma. Here, we demonstrate that down-regulation of GPx3 in the plasma of obese subjects is associated with adipose GPx3 dysregulation, resulting from the increase of inflammatory signals and oxidative stress. Although GPx3 was abundantly expressed in kidney, lung, and adipose tissue, we observed that GPx3 expression was reduced selectively in the adipose tissue of several obese animal models as decreasing plasma GPx3 level. Adipose GPx3 expression was greatly suppressed by prooxidative conditions such as high levels of TNFα and hypoxia. In contrast, the antioxidant *N*-acetyl cysteine and the antidiabetic drug rosiglitazone increased adipose GPx3 expression in obese and diabetic *db/db* mice. Moreover, GPx3 overexpression in adipocytes improved high glucose-induced insulin resistance and attenuated inflammatory gene expression whereas GPx3 neutralization in adipocytes promoted expression of proinflammatory genes. Taken together, these data suggest that suppression of GPx3 expression in the adipose tissue of obese subjects might constitute a vicious cycle to expand local reactive oxygen species accumulation in adipose tissue potentially into systemic oxidative stress and obesity-related metabolic complications. (*Molecular Endocrinology* 22: 2176–2189, 2008)

ADIPOSE TISSUE contributes to maintaining the energy homeostasis of the whole body not only by buffering lipid metabolites but also by secreting several adipocytokines in response to the inputs of the central nervous system and periphery (1). In obesity, however, adipose tissue fails to accommodate fatty acids effectively according to the changing metabolic requirements, resulting in excessive accumulation of lipid metabolites in peripheral tissues, including the liver and muscle tissues, along with adipocytokine dysregulation (2). The abnormal regulation of adipocytokines occurring in obesity affects the functions of other tissues, including the liver, muscle, central nervous system, and vasculatures, thus increasing the risks for metabolic complications. Therefore, it appears that examining the molecular regulatory mechanisms for adipocytokines in obesity is crucial for understanding metabolic disorders and for developing effective therapeutic interventions for obesity and its related complications.

One of the main clinical manifestations of obesity is increased systemic oxidative stress (3–5). Oxidative stress has been implicated in several forms of tissue damage and leads to pathological conditions such as irradiation damage and ischemia reperfusion injury, as well as neurodegenerative diseases (6, 7). However, accumulating evidence indicates that increased oxidative stress is also strongly associated with metabolic disorders, including atherosclerosis, thrombosis, liver steatosis, and diabetes mellitus, which are often observed in morbid obesity (8–11). Reactive oxygen species (ROS) can rapidly inactivate vascular nitrogen oxide (NO), a major vasorelaxant and inhibitor of platelet function, and can increase the risks for atherosclerosis and stroke. Moreover, posttranslational modifications of fibrinogen by ROS and NO-derived oxidants enhance fibrinogen activity, thus accelerating clot formation and thrombosis (12, 13). In addition, oxidative stress impairs insulin secretion by the pancreatic

First Published Online June 18, 2008

Abbreviations: BAT, Brown adipose tissue; CAT, catalase; ChIP, chromatin immunoprecipitation; f, forward; GPx3, glutathione peroxidase 3; iNOS, inducible nitric oxide synthase; LPO, lipid peroxidation; LPS, lipopolysaccharide; NAC, *N*-acetyl cysteine; NADPH, reduced nicotinamide adenine dinucleotide phosphate; PPAR, peroxisomal proliferator-activated receptor; PPRE, PPAR response element; r, reverse; ROS, reactive oxygen species; RXR, retinoid X receptor; SVC, stromal vascular cell; TBARS, thiobarbituric acid-reactive substances; TZD, thiazolidinedione; WAT, white adipose tissue.

***Molecular Endocrinology* is published monthly by The Endocrine Society (http://www.endo-society.org), the foremost professional society serving the endocrine community.**